Communications in Transportation Research 5 (2025) 100220

Contents lists available at ScienceDirect

Communications in Transportation Research

journal homepage: www.journals.elsevier.com/communications-in-transportation-research

Full Length Article

Efficient and stable ride-pooling through a multi-level coalition formation game

Yaotian Tan[a], Shuyue Qian[a], Aoyong Li[a,*], Haiyang Yu[a], Jie Gao[b]

[a] State Key Lab of Intelligent Transportation System, School of Transportation Science and Engineering, Beihang University, Beijing, 100191, China
[b] Department of Transport & Planning, TU Delft, Delft, 2628 CN, the Netherlands

ARTICLE INFO

Keywords:
Ride-pooling
Stable matching
Coalition formation
Game theory

ABSTRACT

Ride-pooling has the potential to offer a sustainable solution for urban mobility by reducing vehicle use and emissions through shared trips. However, its adoption remains limited due to poor matching performance. Many requests fail to form feasible pools, and even successful matches often involve long detours or minimal cost savings. These inefficiencies largely arise from fragmented market structures: most operators act independently, restricting matching to their own request pools and limiting the formation of beneficial coalitions. Aggregation platforms improve efficiency by integrating regional operators through unified dispatch systems, but raise concerns over long-term stability. Differences in operator cost structures and market shares may incentivize deviation, at the same time, passengers may reject assigned payments if more attractive alternatives exist. To address these challenges, we propose a multi-level coalition formation game that jointly models operator and passenger collaboration. At the upper level, operators play a non-cooperative game to decide coalition partners. At the lower level, passengers are grouped into shared trips through a cooperative game that ensures individually rational payments. The two layers are coupled via constraint propagation, forming a unified decision-making process. We evaluate our framework using real-world data from three Chinese regions—Chengdu, Haikou, and the Ningxia Hui Autonomous Region—chosen to reflect diverse urban and regional contexts. Compared to independent operations, our approach increases vehicle occupancy by 14%–28%, reduces total costs by 10%–15%, and shortens average travel distances by 4%–5%. The system maintains stable coalition structures with operator deviation rates below 6.81% and near-zero passenger deviation rates.

1. Introduction

Ride-pooling has emerged as a promising mode of on-demand mobility, offering an efficient and sustainable solution for urban transportation. Unlike traditional ridesharing programs such as carpooling or dial-a-ride, which rely on non-dedicated drivers following personal trip plans, ride-pooling services are managed by centralized platforms and fulfilled by full-time drivers. Well-known examples include UberPool, Lyft Line, GrabShare, and DiDi Express Pool (Ke et al., 2020). These services match multiple passengers with similar trips to share a vehicle and divide the cost, resulting in what is referred to in game-theoretic terms as a passenger coalition (Bistaffa et al., 2017). By increasing vehicle utilization, ride-pooling is expected to ease traffic congestion and decrease emissions. In a simulation based on DiDi's operational data, Zhu and Mo (2022) estimated that large-scale ride-pooling in Haikou could reduce vehicle kilometers traveled (VKT) by over 8%, saving more than 1.2 million L of fuel and 3300 t of CO_2 annually.

Despite its many advantages, ride-pooling adoption remains low, accounting for less than 30% of ride-hailing trips in many cities (Li et al., 2019). A key barrier is the limited effectiveness of matching: Many requests fail to form feasible passenger coalitions, and even successful ones often involve long detours and suboptimal routing, weakening the cost advantage of ride-pooling (Ke et al., 2020). These problems are largely driven by the fragmented and competitive ride-pooling market structure. By October 2024, a total of 362 ride-hailing operators in China had obtained official licenses, many of which provide both solo and pooling services (Feng et al., 2024; MOT, 2024). However, these operators typically act independently and restrict matching within their own request pools (Liu et al., 2023; Zhou et al., 2022), limiting the space of feasible coalitions and reducing the potential for efficient pooling. Despite adequate demand in many areas, the lack of coordination fragments the matching process. Passengers may experience long

* Corresponding author.
E-mail address: liaoyong@buaa.edu.cn (A. Li).

https://doi.org/10.1016/j.commtr.2025.100220
Received 4 June 2025; Received in revised form 2 September 2025; Accepted 3 September 2025
Available online 15 November 2025

Nomenclature

Notation	Definition
Set	
N, N^o, N^p	Sets of all agents, operators, and passengers
C, C^o, C^p	Coalition, operator coalition, and passenger coalition
$\mathcal{CS}, \mathcal{CS}^o, \mathcal{CS}^p$	Coalition structure, operator coalition structure, and passenger coalition structure
$\mathcal{VC}$	Set of valid passenger coalitions
$\mathcal{VR}$	Set of valid routes
$\mathcal{DG}$	Set of deviation groups
Utility	
x_i	Utility allocated to operator i (revenue)
y_i	Utility allocated to passenger i (negative payment)
s_{ij}	Surplus of passenger i over j
$u(C^o)$	Operator coalition utility
$u(C^p)$	Passenger coalition utility
$g(C^o)$	Deviation gain of operator coalition C^o
$\delta(C^p)$	Maximum surplus difference of passenger coalition C^p
Graph	
$G^p = (N^p, E^p)$	Passenger graph
$G^g = (N^g, E^g)$	Geographical graph
n_i^o, n_i^o	Pick-up and drop-off points of passenger i
R	Vehicle route
$d(R)$	Travel distance of route R
$c(R)$	Operating cost of route R
Parameter	
λ	Vehicle capacity excluding the driver (pax/veh)
ρ	Profit parameter (CNY/km)
γ	Cooperative benefit parameter (pax/veh)
ϵ	Convergence tolerance of CRP–CFSS
τ	Time limit in CRP–CFOS (s)
w_i	Investment weight of operator i
c^f, c^e, c^d	Fuel, employment and depreciation cost (CNY/km)
Abbreviation	
CRP	Coalitional ride-pooling program
CSG	Coalition structure generation
GCCF	Graph-constrained coalition formation
CFSS	Coalition formation with sparse synergies
CFOS	Coalition formation for operator stability
PK	Payments in the kernel

waiting times and unsatisfactory matches, with circuitous routes and only limited cost savings. Such inefficiencies reduce user satisfaction and make ride-pooling less attractive over time.

A natural solution is to enable cross-operator pooling through coalition formation. Aggregation platforms such as Amap have begun to explore this possibility. By integrating regional operators (e.g., 6 in Beijing and up to 26 in Chongqing), Amap has established a unified dispatch platform where participating operators jointly serve incoming requests, regardless of the submission channel (Hou et al., 2025a; Liu et al., 2024; Ma et al., 2025). Unlike ride-hailing services, where passengers may choose a preferred operator, ride-pooling platforms typically do not offer such options. This corresponds to a grand coalition structure, where all operators form a unified coalition to jointly process all requests. While this arrangement improves overall efficiency, it raises concerns about long-term stability. Differences in operator size, market share, and cost structure make it difficult to ensure that all participants continue to benefit. If an operator finds it more profitable to act independently or within a smaller coalition, it may choose to deviate, undermining the stability of the grand coalition structure (Liu et al., 2024). For example, Baidu's ride-pooling platform initially integrated multiple operators but now works exclusively with Didi.

At the same time, stability concerns also arise on the passenger side. Compared to users of ride-hailing services, ride-pooling passengers are generally more sensitive to their assigned payments (Alonso-González et al., 2020). Passengers with more attractive alternatives may expect lower payments and reject pooling options that do not reflect their perceived bargaining power. While this issue has been widely studied in recent years (Bistaffa et al., 2017; Lu and Quadrifoglio, 2019; Wang et al., 2018), it becomes even more pronounced under aggregation modes, where operator coalitions expand the range of feasible passenger coalitions and increase the likelihood that passengers perceive more attractive alternatives.

To address these challenges, we propose a multi-level game framework that focuses on two core tasks: operator coalition formation and passenger coalition formation. Guided by differences in coalition autonomy and utility transferability, we model operator coalition formation as a non-cooperative game and passenger coalition formation as a cooperative game. At the upper level, operators decide whether and with whom to collaborate through a shared dispatch platform for pooling services. At the lower level, passengers are grouped into shared trips based on routing feasibility and cost-effectiveness. The two layers are coupled: Operator coalitions determine the space of feasible passenger coalitions, while the resulting passenger coalitions influence operator revenues and coalition incentives. In both layers, stability is ensured through utility allocation, which distributes total revenue among participating operators and assigns individual payments to passengers in a fair and stable manner.

Specifically, the contributions of this study are as follows:

- We propose a dynamic coalition formation method that enables operators to form coalitions based on real-time travel requests, as opposed to static scenarios of full competition or full cooperation. This method adapts to changing conditions and ensures both efficiency and stability in ride-pooling systems.
- We introduce a multi-level game framework that separately models the decision-making processes of both operators and passengers in ride-pooling matching, achieving stable outcomes for both parties. To the best of our knowledge, this is the first work to address the stability of operator and passenger matchings simultaneously.
- We propose a series of algorithms to address the combinatorial explosion in coalition formation, and validate the proposed framework through experiments conducted in three representative regions in China. The results demonstrate significant improvements in vehicle occupancy, total costs, and average travel distances, with operator deviation rates maintained below 6.81% and near-zero passenger deviations.

The remainder of this paper is structured as follows. Section 2 reviews the related literature. Section 3 defines the problem and proposes the formal framework. Section 4 develops the coalition formation algorithms, followed by the utility allocation algorithms proposed in Section 5. Section 6 presents a case study. Finally, Section 7 summarizes the findings and potential future work.

2. Literature review

Passenger matching has been extensively studied in both ridesharing and ride-pooling contexts. In ridesharing, where drivers are non-dedicated and follow personal trip plans, the focus is typically on pairing passengers with suitable drivers. In contrast, ride-pooling services are managed by centralized platforms and rely on full-time drivers. Matching in this setting occurs primarily among passengers, who are more concerned about whom they share the ride with, as well as the resulting detour and payment.

A common strategy in both contexts is optimal matching, which aims to maximize system efficiency and resource utilization (Li et al., 2024; Liu et al., 2022; Wei et al., 2022). However, this approach often assumes full passenger compliance, which rarely holds in practice (Hou et al., 2025b). Passengers may reject assigned matches if they find them inconvenient or inequitable (Wang et al., 2018), underscoring the need for stability. Existing studies address this issue from two perspectives. One is preference-based stability, which accounts for individual factors such as gender, privacy concerns, and ride history (Cui et al., 2020; Gao et al., 2022; Tang et al., 2022; Zhang and Zhao, 2019). The other is payment-based stability, which is also the focus of our study and ensures

that no passenger has an incentive to deviate under a given payment (Bistaffa et al., 2017; Lu and Quadrifoglio, 2019; Yao and Bekhor, 2023).

In Sections 2.1 and 2.2, we review relevant cooperative and non-cooperative game approaches for designing payment-stable matchings. To further extend the matching problem from passengers to operators, we examine inter-operator dynamics in aggregation platforms and the corresponding coalition formation mechanisms in Section 2.3.

2.1. Stable matching based on cooperative games

The cooperative game paradigm follows a "match first, then price" strategy, where the optimal matching scheme is determined first, and solution concepts from cooperative game theory (e.g., core, kernel, nucleolus, and Shapley value) are subsequently applied to ensure stable payments. Bistaffa et al. (2015a, 2015b, 2017) developed a coalition formation model constrained by social networks and proposed a method for computing kernel-stable payments. Lu and Quadrifoglio (2019) and Tae et al. (2020) minimized the maximum passenger dissatisfaction by computing the nucleolus, demonstrating its feasibility under non-empty core conditions. Chremos and Malikopoulos (2021) analyzed passenger-vehicle assignment and stable profit allocation using binary linear programming, showing that core-based schemes ensure individual rationality. In the context of dynamic matching, Ke et al. (2025) incorporated the concepts of core, nucleolus, and Shapley values into a rolling decision framework to improve stability over time.

While the core is widely used, it does not always exist and is computationally intractable in large-scale settings. The nucleolus guarantees fairness but depends on a non-empty core and requires solving a sequence of linear programs. The Shapley value ensures uniqueness but may violate individual rationality in decentralized environments. In this study, we adopt the concept of the kernel to define passenger-level stability. Compared to other notions, the kernel captures pairwise bargaining dynamics and offers a better balance between stability and computational efficiency, making it well suited for real-world ride-pooling systems (Chalkiadakis et al., 2016; Davis and Maschler, 1965; Wooldridge, 2011).

2.2. Stable matching based on non-cooperative games

In the non-cooperative game paradigm, matching and pricing occur simultaneously. Each matching scheme corresponds to a payment arrangement defined by a payment-splitting mechanism (e.g., static protocols and dynamic auctions), with stability achieved at equilibrium. These approaches can be categorized into centralized and decentralized methods. Centralized methods achieve equilibrium through unified decision making. Wang et al. (2018) employed mathematical programming to obtain nearly stable matches under incomplete and dynamic information settings. Peng et al. (2020) proposed a stable ridesharing model based on the deferred acceptance algorithm, minimizing commuting costs while ensuring fair incentives. Fielbaum et al. (2022) developed novel cost-sharing protocols that transform the optimal matching solution into equilibrium, addressing the inherent trade-off between efficiency and individual rationality. In contrast, decentralized methods allow participants to make decisions based on local interactions and information. Nourinejad and Roorda (2016) introduced an agent-based dynamic auction mechanism to achieve near-optimal and stable matching with reduced computational complexity. Chau et al. (2022) designed a decentralized ridesharing scheme with fair cost splitting, ensuring stability without centralized coordination.

Most existing models are built upon the concept of Nash Equilibrium (NE), which only guards against unilateral deviations. However, in settings where operators can cooperate, such a notion is insufficient. To better capture coalition-level incentives, we adopt the concept of Strong Nash Equilibrium (SNE) to define operator-level stability. Unlike the standard version, SNE prevents coordinated deviations by any subset of operators, making it particularly suited for modeling cooperative behaviors in multi-operator systems (Fielbaum et al., 2022).

2.3. Operator relationships on aggregation platforms

The rise of aggregation platforms has reshaped the competitive and cooperative relationships among ride-pooling operators. Liu et al. (2024) found that user single-homing and multi-homing significantly influence platform competition, with price signaling potentially triggering asymmetric market dynamics. Cai et al. (2024) demonstrated that strategic adjustments in prices and commissions could lead to a dynamic equilibrium in ride-pooling markets. These studies provide valuable insights into operator interactions within an aggregation framework. While this setting improves resource utilization, Ma et al. (2025) revealed its inherent instability: smaller operators face marginalization due to imbalanced revenue allocation, and operators may deviate if equilibrium is not achieved. To address these challenges, we propose a dynamic coalition formation mechanism that selectively partitions operators into coalitions based on real-time travel requests. This mechanism mitigates the "winner-takes-all" effect observed in grand coalition systems while preserving high matching efficiency.

To summarize, existing literature has advanced passenger-level stable matching with robust game-theoretic frameworks. However, while research on aggregation platforms has examined both competitive and cooperative dynamics, it has not addressed how to sustain stable cooperation among operators—a critical gap given the risk of deviations under imbalanced allocations. Moreover, operator collaboration expands feasible passenger coalitions via cross-operator pooling, increasing passengers' access to alternatives and amplifying passenger stability challenges. Our work fills these gaps by jointly modeling stability dynamics at both the operator and passenger layers.

3. Problem formulation

3.1. Basic definitions

In game theory, a coalition $C \subseteq N$ is a subset of agents that cooperate to achieve greater utility, where N denotes the set of all agents. A coalition structure $\mathcal{CS} = \{C_1, C_2, \ldots, C_K\}$ is a partition of N, where $K \in \mathbb{Z}^+$ denotes the total number of coalitions. Each subset $C_k \in \mathcal{CS}$ (with $k = 1, 2, \ldots, K$) denotes a coalition and satisfies $\forall k \neq l : \bigcup_{k=1}^{K} C_k = N \wedge C_k \cap C_l = \varnothing$, which ensures all agents are included and no agent belongs to multiple coalitions. The function $u(C) : 2^N \to \mathbb{R}$ quantifies the total utility of coalition C, where 2^N includes all possible coalitions, and $\mathbb{R}$ denotes the real field. Building upon these foundations, we introduce the relevant concepts of ride-pooling at the operator and passenger level, respectively.

3.1.1. Operator level

Definition 1. **(Operator coalition)** An operator coalition $C^o \subseteq N^o$ is a group of operators that jointly serve a shared pool of travel requests, where N^o denotes the set of all operators. The utility of C^o, denoted $u(C^o)$, refers to the total revenue it generates and is allocated among members such that $u(C^o) = \sum_{i \in C^o} x_i$, where x_i is the share received by operator $i \in C^o$.

The operator coalition structure is denoted as $\mathcal{CS}^o$, with utility $u(\mathcal{CS}^o) = \sum_{C^o \in \mathcal{CS}^o} u(C^o)$. The number of such possible structures equals the Bell number $B_{|N^o|}$, which is defined by the recursive formula $B_{|N^o|} = \sum_{k=0}^{|N^o|-1} \binom{|N^o|-1}{k} B_k$ with the base case $B_0 = 1$ (Berend and Tassa, 2010). This results in an exponential growth in the number of possible coalition structures as the number of operators $|N^o|$ increases, leading to a combinatorial explosion that significantly raises computational complexity.

To capture the emergence of such structures in decentralized environments, we model the coalition formation process as a non-cooperative game. Although operators collaborate within each coalition, their decisions are made independently—each operator selects potential partners without relying on centralized coordination. Once a coalition is formed, its total utility is divided among members based on individual attributes, following a predetermined rule shared across the system. As this allocation is fixed and exogenous to the coalition formation process, utilities are considered non-transferable among members, as formally stated in Assumption 1.

Assumption 1. **(Utilities among operators are non-transferable)** Given a coalition structure $\mathcal{CS}^o$, the utility allocation $X = (x_1, x_2, \ldots, x_{|N^o|})$ is determined by a certain fixed protocol (see Section 5.1) and is not transferable among operators.

Given the non-transferable nature of utilities, some coalitions may have incentives to deviate and regroup for higher individual utilities, which motivates the concept of stable operator coalition structure.

Definition 2. **(Stable operator coalition structure)** An operator coalition structure $\mathcal{CS}^o$ is said to be stable (denoted as $\mathcal{CS}^o_{\text{st}}$) if the corresponding allocation $X = \{x_i\}_{i \in N^o}$ satisfies the following condition:

$$\sum_{i \in C^o_b} x_i \geq u\left(C^o_b\right), \quad \forall C^o_b \subseteq N^o, C^o_b \neq \varnothing \tag{1}$$

where C^o_b denotes any potential subset (coalition) of operators, and $u\left(C^o_b\right)$ is the total utility that coalition C^o_b can generate by operating independently. To illustrate, consider three operators $N^o = \{1, 2, 3\}$ with a coalition structure $\mathcal{CS}^o = \{\{1, 2\}, \{3\}\}$ and allocation $X = (x_1 = 4, x_2 = 4, x_3 = 4)$. Suppose a potential deviating coalition $\{1, 3\}$ can generate utility $u(\{1, 3\}) = 9$. Since $x_1 + x_3 = 8 < 9$, the structure is unstable as $\{1, 3\}$ would deviate.

Definition 2 adopts the concept of Strong Nash Equilibrium (SNE), which ensures group-level stability: no group of operators has an incentive to deviate and form a separate coalition. As a direct implication, such a stable structure also satisfies individual rationality, meaning that each operator receives at least as much utility as they could secure on their own. This condition ensures that participation in the coalition is voluntary and beneficial for every operator.

Proposition 1. *Any stable operator coalition structure $\mathcal{CS}^o_{\text{st}}$ satisfies individual rationality. That is, for each operator $i \in N^o$, we have*

$$x_i \geq u(\{i\}) \tag{2}$$

where x_i denotes the utility that operator i receives under the coalition structure, and $u(\{i\})$ is the utility that operator i can achieve when operating independently. Notice that a SNE does not always exist, and verifying its existence is computationally challenging (Fielbaum et al., 2022). In cases where no SNE exists, the structure that minimizes the total deviation gain is regarded as approximately stable, with details provided in Section 4.2.

3.1.2. Passenger level

The operator coalition structure $\mathcal{CS}^o$ directly influences the space of passenger matching. To illustrate this, consider a passenger graph $G^p = (N^p, E^p)$, where N^p represents all passengers, and $E^p \subseteq N^p \times N^p$ indicates potential pooling relationships. Specifically, passengers i and j can share a vehicle, i.e., $(i, j) \in E^p$, if and only if the operators they select belong to the same operator coalition. Fig. 1 provides an example of the passenger graph.

Definition 3. **(Passenger coalition)** A passenger coalition $C^p \subseteq N^p$ is a group of passengers sharing a vehicle, where N^p denotes the set of all passengers. The set of valid passenger coalitions $\mathcal{VC}(\mathcal{CS}^o, \lambda)$ includes all C^p satisfying

- Capacity constraint: $1 \leq |C^p| \leq \lambda$, where λ is vehicle capacity excluding the driver.
- Operator constraint: The induced subgraph $G^p(C^p)$ is complete, i.e., $\forall i, j \in C^p$: $(i, j) \in E^p$.

The utility of C^p, denoted $u(C^p)$, refers to the total cost savings achieved through pooling, and satisfies $u(C^p) = \sum_{i \in C^p} \left(c_i^{\text{solo}} - p_i\right)$, where c_i^{solo} is the solo travel cost and p_i is the pooling payment. As c_i^{solo} is fixed and independent of coalition formation, we simplify $u(C^p) = -\sum_{i \in C^p} p_i$. This utility is allocated among members such that $u(C^p) = \sum_{i \in C^p} y_i$, where y_i is the utility assigned to passenger i, equal to the negative of their payment.

The passenger coalition structure is denoted as $\mathcal{CS}^p$, which satisfies $\forall C^p \in \mathcal{CS}^p : C^p \in \mathcal{VC}$, and has utility $u(\mathcal{CS}^p) = \sum_{C^p \in \mathcal{CS}^p} u(C^p)$. Unlike operators, passengers have limited autonomy in forming coalitions. Their grouping is determined by operators aiming to minimize total operating costs, leading to the identification of the optimal passenger coalition structure:

$$\mathcal{CS}^p_* = \arg\max_{\mathcal{CS}^p} \sum_{C^p \in \mathcal{CS}^p} u(C^p) \tag{3}$$

Each operator coalition structure $\mathcal{CS}^o$ uniquely determines a corresponding optimal passenger coalition structure $\mathcal{CS}^p_*$, with two induced mappings:

- $f^{\rightarrow}_{p,o} : \mathcal{CS}^p_* \rightarrow \mathcal{CS}^o$ is surjective but not injective, mapping each passenger coalition C^p to the operator coalition C^o that serves it;
- $f^{\rightarrow}_{o,p} : \mathcal{CS}^o \rightarrow \mathcal{CS}^p_*$ is bijective, mapping each operator coalition C^o to the set of passenger coalitions it serves.

Since utility allocation among passengers essentially determines

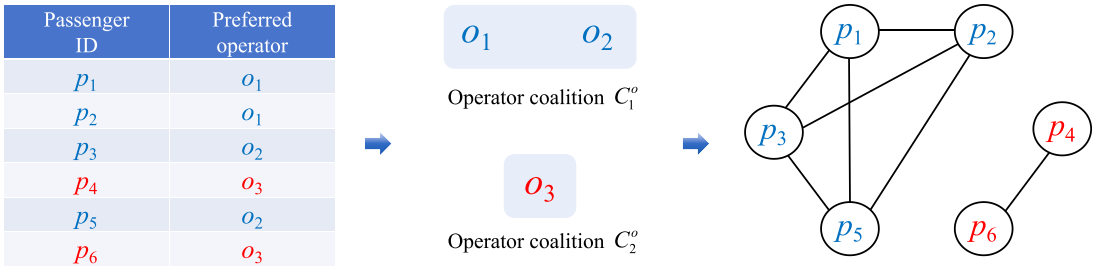

(a) Travel request submit (b) Operator coalition structure (c) Passenger graph

Fig. 1. Example of passenger graph. Passengers first submit requests to their preferred operators. Given the operator coalition structure $\mathcal{CS}^o = \{\{o_1, o_2\}, \{o_3\}\}$, passengers p_1, p_2, p_3, p_5 are served by coalition $\{o_1, o_2\}$ and passengers p_4, p_6 by $\{o_3\}$.

their payments and is managed by operators, we adopt the following assumption.

Assumption 2. **(Utilities among passengers are transferable)** Given a passenger coalition structure $\mathcal{CS}^p$, the utility of each coalition $C^p \in \mathcal{CS}^p$ can be freely transferred among its members.

Assumption 2 allows us to maintain stability through internal reallocations within coalitions without altering $\mathcal{CS}^p_s$, aligning with the cooperative game paradigm. As passengers only compare their allocated utilities with others in the same coalition, it is sufficient to ensure stability within each individual coalition. We adopt the ϵ-kernel condition to capture this internal stability: it limits dissatisfaction among members and provides a relaxed yet practical alternative to core stability, which is often too stringent in real-world pooling (Deng and Papadimitriou, 1994; Greco et al., 2011; Klusch and Shehory, 1996).

Definition 4. **(Stable passenger coalition structure)** A passenger coalition structure $\mathcal{CS}^p$ is said to be stable (denoted as $\mathcal{CS}^p_{\text{st}}$) if there exists an allocation $Y = \{y_i\}_{i \in N^p}$ such that, for any $C^p \in \mathcal{CS}^p$, the following condition holds

$$\frac{\delta(C^p)}{|u(\mathcal{CS}^p)|} \leq \epsilon \tag{4}$$

where

$$\delta(C^p) = \max_{i,j \in C^p} (s_{ij} - s_{ji}) \tag{5}$$

$$s_{ij} = \max_{C^p_b \in \mathcal{VC}} \left\{ u(C^p_b) - \sum_{k \in C^p_b} y_k \;\middle|\; i \in C^p_b,\ j \notin C^p_b \right\} \tag{6}$$

To illustrate, consider three passengers $N^p = \{1, 2, 3\}$ forming $C^p = \{1, 2, 3\}$ with $u(C^p) = -15$ and allocation $Y = (-2, -5, -8)$. Suppose $u(\{1\}) = -3$, $u(\{3\}) = -5$, $u(\{2, 3\}) = -11$, $u(\{1, 2\}) = -9$. For the pair $(3, 1)$, $s_{31} = \max\{u(\{3\}) - y_3, u(\{2, 3\}) - (y_2 + y_3)\} = 3$, and $s_{13} = \max\{u(\{1\}) - y_1, u(\{1, 2\}) - (y_1 + y_2)\} = -1$. Hence $\delta(C^p) \geq s_{31} - s_{13} = 4$. With $\epsilon = 0.1$, $\delta(C^p)/|u(C^p)| \geq 4/15 \approx 0.27 > 0.1$, so the coalition is not ϵ-kernel stable.

Remark. **(Connection to ϵ-kernel stability)** The stability condition in Definition 4 is inspired by the ϵ-kernel concept in cooperative game theory (Klusch and Shehory, 1996), which bounds internal surplus imbalances among agents to ensure approximate core stability. Here, we adopt a similar approach to limit relative dissatisfaction within each coalition. This relaxed form of stability is particularly suitable for centralized ride-pooling platforms, where passengers do not engage in active negotiation but implicitly assess fairness based on assigned utility.

We have defined stability separately for operators and passengers. For passengers, limited autonomy and transferable utilities enable modeling via cooperative game theory, where platforms first identify cost-minimizing optimal coalition structures (ensuring collective rationality), then allocate costs via utility transfers to set payments that prevent passenger deviations (ensuring individual rationality). For operators, autonomy and non-transferable revenues necessitate non-cooperative game theory, where revenue allocations are tied to specific coalition structures. Here, optimal coalition structures cannot be pre-guaranteed; instead, stability is achieved by adjusting structures to ensure allocations meet individual rationality. We now proceed to Section 3.2, which presents a practical framework based on these concepts.

3.2. Formal framework

In this section, we introduce the coalitional ride-pooling program (CRP), a framework designed to promote efficient and stable ride-pooling through multi-level games. In practice, this framework could be managed by an aggregation platform, referred to as the CRP Hub.

As shown in Fig. 2, passengers can submit their travel requests either through the official app of their preferred operators or directly through the CRP Hub. If submitted via operator apps, passengers can explicitly indicate whether they wish to join CRP. Requests with such intent are forwarded to the CRP Hub, while others are handled by operators independently. For requests submitted directly to the CRP Hub, passengers may specify their preferred operator and are automatically enrolled in CRP. At the same time, vehicles report real-time statuses to their affiliated operators, which are also collected by the CRP Hub.

After gathering these inputs, the CRP Hub performs coalition formation to determine partnership groups for operators and passengers, respectively. During this process, coalition utilities are allocated within each coalition—this allocation guides the formation of coalitions by ensuring stable structures, with no operator or passenger incentivized to deviate (see Section 4.1 for details on coalition utility). Based on this process, the CRP Hub generates orders, each containing two types of menus directed to different parties:

- **Operator menu**, which includes a stable operator coalition structure $\mathcal{CS}^o_{\text{st}}$ and the corresponding allocation $X = (x_1, x_2, \ldots, x_{|N^o|})$. These specify which operators form temporary cooperation and how revenue is allocated, respectively.

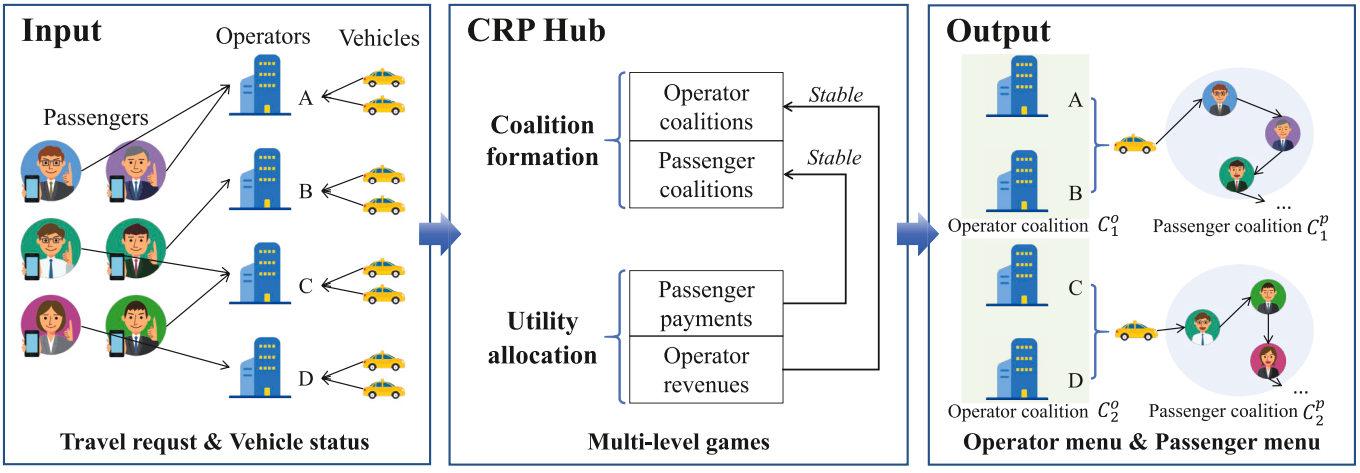

Fig. 2. Overview of the CRP framework. In this example, Operators A and B form coalition $\mathcal{C}^o_1$ and dispatch the nearest vehicle for passenger coalition $\mathcal{C}^p_1$, while Operators C and D form $\mathcal{C}^o_2$ for $\mathcal{C}^p_2$.

- **Passenger menu**, which includes the optimal passenger coalition structure $\mathcal{CS}^p_*$ constrained by $\mathcal{CS}^o_{st}$ and an allocation $Y = (y_1, y_2, \ldots, y_{|N^p|})$ ensuring $\mathcal{CS}^p_* = \mathcal{CS}^p_{st}$. These specify which passengers share rides and how they split the payment, respectively.

Once an order is generated, the operator menu is sent to the corresponding operators for vehicle dispatching, while the passenger menu is sent to the corresponding passengers for order confirmation. There are four types of entities in CRP, i.e., operators, passengers, vehicles, and the CRP Hub. Fig. 3 illustrates how these entities interact under the coordination of the CRP Hub. Specifically, the CRP Hub generates orders through the following batch-processing steps:

1) Initialize iteration counter $t = 0$.
2) Generate current operator coalition structure $\mathcal{CS}^o(t)$ (initial structure for $t = 0$; adjusted structure for $t \geq 1$).
3) Determine the set of valid passenger coalitions $\mathcal{VC}(\mathcal{CS}^o(t), \lambda)$ based on $\mathcal{CS}^o(t)$ and vehicle capacity λ.
4) Compute optimal passenger coalition structure $\mathcal{CS}^p_*(t)$ under $\mathcal{VC}(\mathcal{CS}^o(t), \lambda)$. The time for single execution shall not exceed τ; output the best current approximate solution if timeout occurs. This step involves solving vehicle routing problems to determine utilities $u(C^p)$ for each passenger coalition $C^p \in \mathcal{VC}$.
5) Calculate utilities $u(C^o)$ for each operator coalition $C^o \in \mathcal{CS}^o(t)$ based on $u(C^p)$ and mapping relationship $\vec{f}_{o,p}$.
6) Allocate operator utilities according to the predefined protocol, obtaining $X(t) = \{x_i\}_{i \in N^o}$.
7) Check stability of $\mathcal{CS}^o(t)$: if not satisfied, set $t = t + 1$ and return to Step 2; if satisfied, proceed to Step 8 and denote the stable structure as $\mathcal{CS}^o_{st} = \mathcal{CS}^o(t)$.
8) Compute exact optimal passenger coalition structure $\mathcal{CS}^p_*$ under $\mathcal{VC}(\mathcal{CS}^o_{st}, \lambda)$ without τ constraint.
9) Iteratively compute ϵ-kernel stable utility allocation $Y = \{y_i\}_{i \in N^p}$ within passenger coalitions to ensure $\mathcal{CS}^p_{st} = \mathcal{CS}^p_*$.
10) Output the final order containing $\mathcal{CS}^o_{st}$, X, $\mathcal{CS}^p_{st}$, and Y.

Several challenges remain unresolved in the above steps, including:

- How to define coalition utility in a way that accurately represents practical conditions and incentives? Given that calculating coalition utility involves vehicle routing, how can this optimization be simplified?
- How to adjust operator coalitions to ensure rapid convergence to stability, and how to design fair and practical allocation protocols for operators?
- How to quickly identify the optimal passenger coalition structure, and how to transfer utilities among passengers to achieve rapid convergence to stability?

These issues are addressed in Sections 4 and 5.

4. Coalition formation

4.1. Coalition utility definition

In game theory, coalition utility plays a foundational role in guiding coalition formation—serving as the core metric that drives agents' decisions to collaborate or deviate. Specifically, it determines whether a coalition structure can remain stable: if the allocated utilities satisfy all agents, the structure is deemed stable. For passenger $i \in N^p$, the pick-up and drop-off points are denoted as n_i^σ and n_i^ω, respectively. We define the traffic network as a geographical graph $G^g = (N^g, E^g)$, where N^g represents the set of pick-up and drop-off points, i.e., $N^g = \{n_i^\sigma, n_i^\omega | i \in N^p\}$, and $E^g \subseteq N^g \times N^g$ denotes edges representing the shortest distance connections between these points. Each edge $(i, j) \in E^g$ has a weight d_{ij}, indicating the distance.

Definition 5. **(Route)** A route R is defined as a sequence of points, i.e., $R = (n_1, n_2, \ldots, n_m)$, where each point $n_i \in N^g$ is a pick-up or drop-off point.

Following Ke et al. (2021), we define the set of valid routes as follows.

Definition 6. **(Set of valid routes)** For a given passenger coalition $C^p \in \mathcal{VC}$, the set of valid routes $\mathcal{VR}(C^p)$ includes routes satisfying the following conditions:

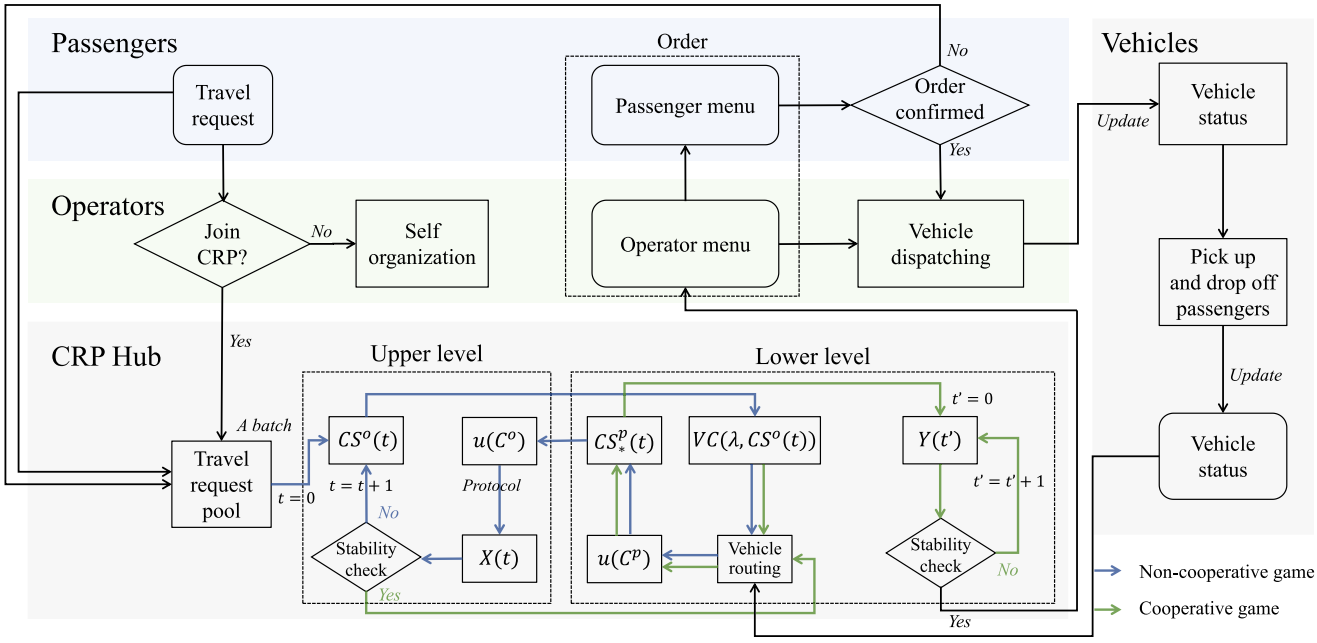

Fig. 3. Interactions and order generation process in CRP.

- Each point in the route must be a pick-up or drop-off point of passengers in C^p, i.e., $\forall k \in 1,2,\ldots,m : R[k] \in \{n_i^\sigma, n_i^\omega | i \in C^p\}$.
- The route must include both pick-up and drop-off points for all passengers in C^p, with each passenger's pick-up point preceding their drop-off point, i.e., $\forall i \in C^p, \exists k_1, k_2 \in 1,2,\ldots,m : R[k_1] = n_i^\sigma, R[k_2] = n_i^\omega, k_1 < k_2$.
- For at least two distinct passengers $i, j \in C^p$ $(i \neq j)$, the pick-up point of j precedes the drop-off point of i, i.e., $\exists k_1, k_2 \in \{1,2,\ldots,m\} : R[k_1] = n_j^\sigma, R[k_2] = n_i^\omega, k_1 < k_2$.

$R \in \mathcal{VR}(C^p)$ denotes a valid route for the vehicle that serves C^p, and examples of such routes are provided in Fig. 4. Assuming sufficient vehicle availability within the service area, Definition 6 simplifies vehicle routing by disregarding vehicle travel from its current position to $R[1]$. Specifically, with operator cooperation, a nearby vehicle can always be dispatched to the first point in the route, making this assumption practical.

Definition 7. **(Optimal route)** The optimal route $R^*_{C^p}$ for passenger coalition C^p is the route $R \in \mathcal{VR}(C^p)$ that minimizes operating cost, i.e.,

$$R^*_{C^p} = \arg\min_{R \in \mathcal{VR}(C^p)} c(R) \tag{7}$$

Following Bistaffa et al. (2017), we define the operating cost as $c(R) = (c^f + c^e + c^d)d(R)$, with $d(R) = \sum_{k=1}^{|R|-1} d_{R[k],R[k+1]}$. Here, c^f, c^e, and c^d represent the fuel cost, employment cost, and depreciation cost parameter, respectively. Since the operating cost directly depends on distance, we simplify the optimal route problem to a shortest route problem, i.e., $R^*_{C^p} = \text{argmin}_{R \in \mathcal{VR}(C^p)} d(R)$, which can be solved efficiently.

Based on the optimal route, the utility of a passenger coalition $C^p \in \mathcal{VC}$ is defined as

$$u(C^p) = -\left(\underbrace{c\left(R^*_{C^p}\right)}_{\text{operating cost}} + \underbrace{\rho \sum_{i \in C^p} d_{n_i^\sigma n_i^\omega}}_{\text{profit part}} \right)_{\text{payment}} \tag{8}$$

Here, the coalition utility equals the negative of total passenger payments (reflecting cost savings from pooling). In addition to covering the operating cost $c\left(R^*_{C^p}\right)$ for the optimal route, the payment includes an additional profit for operators: $\rho \sum_{i \in C^p} d_{n_i^\sigma n_i^\omega}$, where ρ denotes the operator's profit parameter per unit distance.

The utility of the operator coalition $C^o \subseteq N$ is defined as

$$\begin{aligned} u(C^o) &= -\sum_{C^p \in \vec{f}_{o,p}(C^o)} u(C^p)\left(1 + \frac{\gamma\left(D^{\text{single}} - D^{\text{coop}}\right)}{D^{\text{single}}}\right) \\ &= \underbrace{\underbrace{-\sum_{C^p \in \vec{f}_{o,p}(C^o)} u(C^p)}_{\text{total payment}} \underbrace{-\sum_{C^p \in \vec{f}_{o,p}(C^o)} u(C^p)\frac{\gamma\left(D^{\text{single}} - D^{\text{coop}}\right)}{D^{\text{single}}}}_{\text{cooperative benefit}}}_{\text{revenue}} \end{aligned} \tag{9}$$

Here, the operator coalition utility represents the total revenue and comprises two main components:

- **Total payment.** The term $-\sum_{C^p \in \vec{f}_{o,p}(C^o)} u(C^p)$ indicates the total passenger payments served by C^o, which form the short-term base revenue directly derived from current trips.
- **Cooperative benefit.** The term $-\sum_{C^p \in \vec{f}_{o,p}(C^o)} u(C^p)\frac{\gamma\left(D^{\text{single}} - D^{\text{coop}}\right)}{D^{\text{single}}}$ quantifies the long-term revenue potential from improved service quality (e.g., reduced travel distances), which reflects increased demand and sustained earnings growth over time.

where $D^{\text{single}} = \sum_{i \in C^o} \sum_{C^p \in \vec{f}_{o,p}(\{i\})} d\left(R^*_{C^p}\right)$ is the total travel distance when operators in C^o serve passengers independently, and $D^{\text{coop}} = \sum_{C^p \in \vec{f}_{o,p}(C^o)} d\left(R^*_{C^p}\right)$ is the distance when they cooperate. The parameter γ denotes the cooperative benefit per unit of relative distance reduction.

The cooperative benefit quantifies the long-term revenue potential from service quality improvements driven by cooperation, such as reduced travel distances. This value reflects the potential demand growth and sustained earnings growth that arise from enhanced service experiences. It also naturally promotes the superadditivity of $u(\cdot)$ (as defined in Definition 8), supporting coalition formation. Notably, while the operator utility integrates both components to guide coalition formation, the actual monetary distribution among operators (their short-term earnings) is derived solely from the total payment component. The cooperative benefit influences which coalitions are formed but does not directly contribute to the monetary allocations.

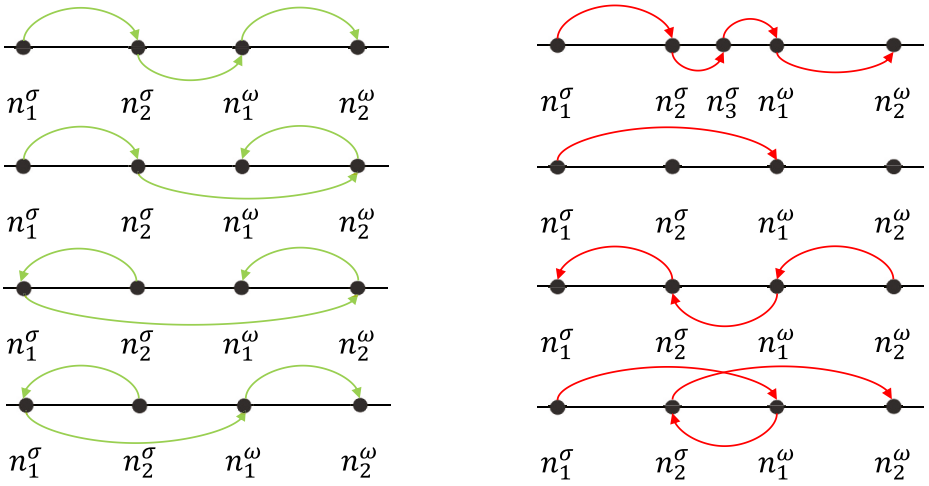

(a) Valid routes (b) Invalid routes

Fig. 4. Examples of valid and invalid routes for the vehicle that serves the passenger coalition $\{p_1, p_2\}$. (b) Four types of invalid routes: (1) visiting a non-member's point; (2) missing pick-up or drop-off points of a member; (3) visiting a drop-off point before the corresponding pick-up; (4) serving requests sequentially without pooling.

Definition 8. **(Superadditivity)** For any two coalitions C_1 and C_2 with $C_1 \cap C_2 = \emptyset$, the function $u(\cdot)$ is superadditive if $u(C_1 \cup C_2) \geq u(C_1) + u(C_2)$.

In general, the utility function $u(\cdot)$ exhibits superadditivity. For passengers, enlarging the matching space usually results in lower payments and higher utility, while for operators, we introduce cooperative benefits to encourage greater cooperation. However, we do not assume strict superadditivity of $u(\cdot)$, as expanding the matching space may sometimes lead to detours, which reduces utility. Therefore, we propose a relaxed property for passenger coalition utility $u(C^p)$: monotonicity.

Proposition 2. *The passenger coalition utility $u(C^p)$ satisfies monotonicity: for any two coalitions $C_1^p \subseteq C_2^p$, it holds that*

$$u(C_1^p) \geq u(C_2^p) \tag{10}$$

Proof. See Appendix A.

Proposition 2 *indicates that if a certain passenger coalition expands further, the payment will increase or stay the same, while its utility will decrease or remain unchanged. This proposition is straightforward and will help to identify the optimal passenger coalition structure in* Section 4.3.

4.2. Operator coalition formation

Identifying the stable operator coalition structure $\mathcal{CS}_{\text{st}}^o$ presents significant computational challenges. First, the number of possible coalition structures grows combinatorially with the number of operators, as quantified by the Bell number $B_{|N^o|}$, making full enumeration infeasible. Second, each potential structure requires solving the optimal passenger coalition structure $\mathcal{CS}_*^p$ as a downstream task—a computationally intensive process. To address these challenges, we propose an iterative algorithm named CRP-CFOS (CRP-coalition formation for operator stability). This approach avoids enumerating all possible structures and reduces iteration counts, efficiently converging to $\mathcal{CS}_{\text{st}}^o$.

4.2.1. Structure initialization

CRP-CFOS begins by assigning all operators to a single coalition, i.e.,

$$\mathcal{CS}^o(t=0) = \{N^o\} \tag{11}$$

The utility $u(C^o)$ for each operator coalition $C^o \in \mathcal{CS}^o(t)$ is computed using Eq. (9), and subsequently, the utility $x_i(t)$ for each operator $i \in C^o$ is determined according to the predefined protocol.

4.2.2. Deviation assessment

For each possible group of operators $C_b^o \subseteq N^o$, the deviation gain is defined as

$$g(C_b^o) = u(C_b^o) - \sum_{i \in C_b^o} x_i(t), \quad \forall C_b^o \subseteq N^o \tag{12}$$

where the deviation gain $g(C_b^o)$ represents the additional utility gained by operators in C_b^o if they form a new coalition.

To reduce iterations, CRP-CFOS adjusts multiple groups simultaneously, rather than a single group at a time. Specifically, it searches for a set of deviation groups $\mathcal{DG}$ defined as

$$\mathcal{DG} = \left\{ C_b^o \subseteq N^o \;\middle|\; C_{b,1}^o \cap C_{b,2}^o = \emptyset,\ \forall C_{b,1}^o, C_{b,2}^o \in \mathcal{DG} \right\} \tag{13}$$

such that the total deviation gain is maximized, i.e.,

$$\mathcal{DG}_{\max} = \arg\max_{\mathcal{DG} \subseteq 2^{N^o}} \sum_{C_b^o \in \mathcal{DG}} g(C_b^o) \tag{14}$$

4.2.3. Structure adjustment

If the total deviation gain $g(\mathcal{CS}^o) = \sum_{C_b^o \in \mathcal{DG}_{\max}} g(C_b^o) \leq 0$, the structure is stable. Otherwise, the coalition structure is updated as

$$\mathcal{CS}^o(t+1) = \left(\mathcal{CS}^o(t) \ominus \bigcup_{C_b^o \in \mathcal{DG}_{\max}} C_b^o \right) \cup \mathcal{DG}_{\max} \tag{15}$$

where the operation $\ominus$ is defined as follows.

Definition 9. **($\ominus$)** Let $\mathcal{CS}$ be a set-cluster and C be a set, then the operation $\mathcal{CS} \ominus C$ is defined as

$$\mathcal{CS} \ominus C = \{\mathcal{A}' | \mathcal{A}' = \mathcal{A} \backslash (\mathcal{A} \cap C), \mathcal{A} \in \mathcal{CS}, \mathcal{A}' \neq \emptyset\} \tag{16}$$

where $\mathcal{A}$ represents any element (a set) in the set-cluster $\mathcal{CS}$, and $\mathcal{A}'$ is the resulting set after removing the intersection of $\mathcal{A}$ and C. This operation effectively removes elements of C from each set in $\mathcal{CS}$ and only retains non-empty sets.

4.2.4. Stopping criterion

Since a Strong Nash Equilibrium may not always exist, we define an additional stopping criterion. If the newly formed coalition structure $\mathcal{CS}^o(t+1)$ has been explored before, the algorithm considers the next-best set of deviation groups with positive gains. This process repeats until no new coalition structure emerges. Then the structure that minimizes the total deviation gain $g(\mathcal{CS}^o)$ is regarded as approximately stable, as no other explored structure exhibits a lower deviation gain.

4.3. Passenger coalition formation

In this section, we identify the optimal passenger coalition structure, which corresponds to the coalition structure generation (CSG) problem in cooperative game theory (Sandholm et al., 1999)—specifically, a graph-constrained coalition formation (GCCF) problem due to the constraints outlined in Definition 3. Unlike operator coalition structures, valid passenger coalitions follow a constrained Bell number due to these constraints. Despite these constraints, computational challenges are far more acute for passengers: their numbers are orders of magnitude larger than operators, making even constrained combinatorial growth intractable (e.g., 20 passengers with standard capacity limits yield over 10^9 valid partitions). In addition, utility calculation for each coalition requires solving a vehicle routing problem.

Coalition formation with sparse synergies (CFSS) is the state-of-the-art algorithm to solve the GCCF problem (Bistaffa et al., 2014). However, applying CFSS to CRP is infeasible due to two reasons: first, CFSS is designed for sparse graph constraints, and second, it requires superadditivity of coalition utilities for pruning. Since coalition utilities in CRP do not always satisfy superadditivity, we propose CRP-CFSS, an adapted version of CFSS that refines the graph constraints and computation to better align with CRP requirements.

4.3.1. Graph constraint

As described in Section 3.1, valid passenger coalitions are constrained by the operator coalition structure, which forms the passenger graph $G^p = (N^p, E^p)$. As shown in Fig. 5, G^p can be decomposed into multiple subgraphs, i.e.,

$$G^p = \bigcup_{k=1}^{m} G_k^p \tag{17}$$

where each subgraph $G_k^p = (N_k^p, E_k^p)$ satisfies the following properties:

- Disjoint, i.e., $\forall k, k' \in \{1, 2, \ldots, m\}, k \neq k' : N_k^p \cap N_{k'}^p = \emptyset$.
- Complete, i.e., $\forall i, j \in N_k^p : (i.j) \in E_k^p$.
- All passengers in N_k^p are served by the operator coalition C_k^o, i.e., $\forall i \in N_k^p : i \in \vec{f_{o,p}}(C_k^o)$.

To avoid repeatedly verifying operator constraints, we restrict the search to each subgraph G_k^p. Thus, the optimal passenger coalition

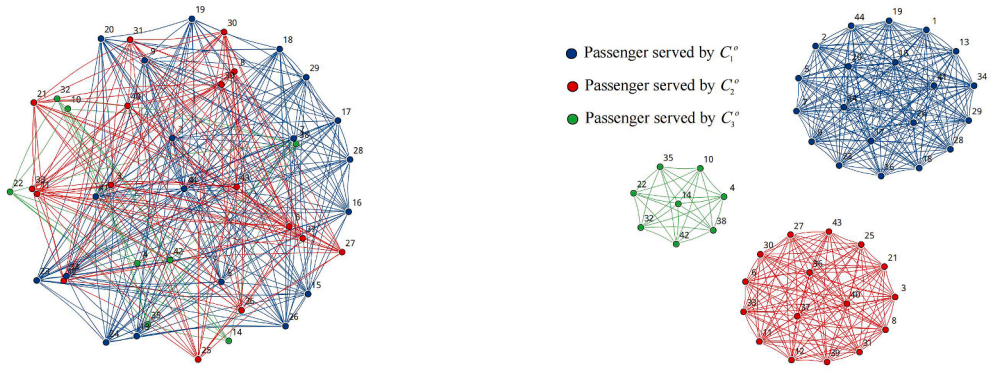

Fig. 5. Example of graph constraint processing.

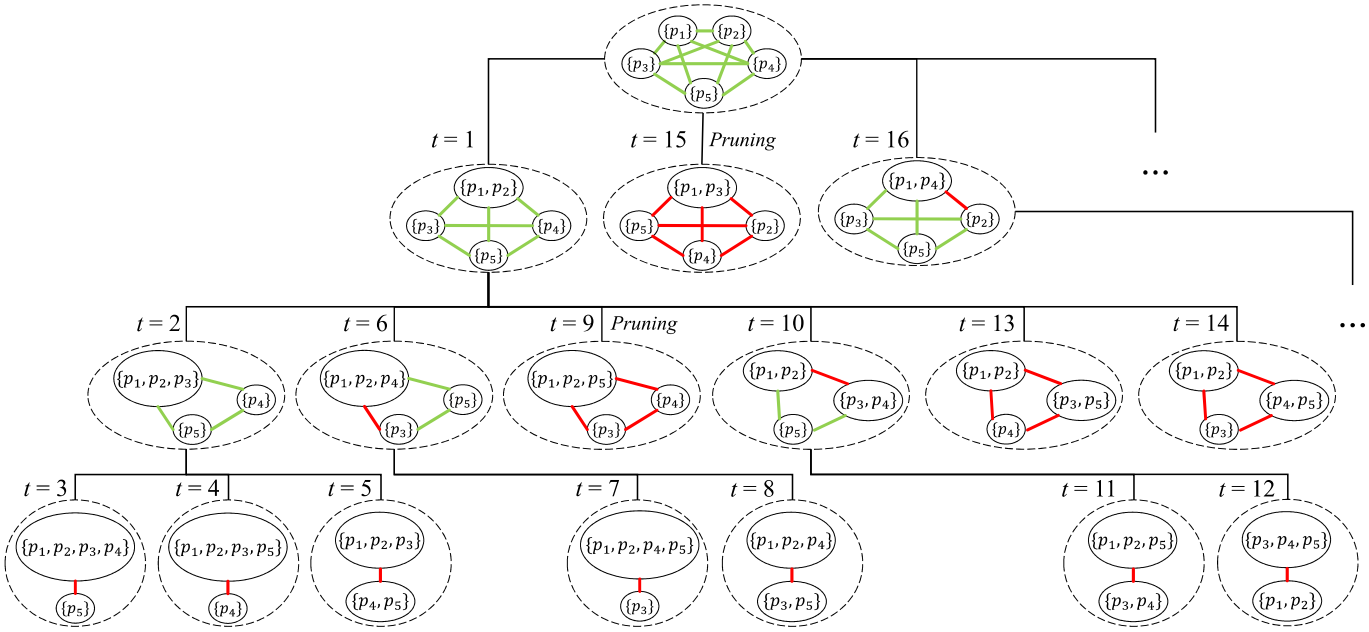

Fig. 6. Schematic of CRP-CFSS algorithm. The vehicle capacity λ is set to 4.

structure $\mathcal{CS}_*^p$ is the union of the optimal substructures $\mathcal{CS}_{k,*}^p$, given by

$$\mathcal{CS}_*^p = \bigcup_{k=1}^{m} \mathcal{CS}_{k,*}^p \tag{18}$$

This decomposition reduces the complexity from $O\left(2^{|N^p|}\right)$ to $O\left(\sum_{k=1}^{m} 2^{|N_k^p|}\right)$, significantly improving search efficiency, particularly when the number of subgraphs m is large.

4.3.2. Structure initialization

As shown in Fig. 6, all edges within each subgraph G_k^p are initially marked green, indicating that passengers connected by these edges can potentially form coalitions. The initial passenger coalition structure is defined as

$$\mathcal{CS}^p(t=0) = \{\{i\} | i \in N_k^p\} \tag{19}$$

where each passenger initially forms their own coalition. This structure serves as the root node ($t = 0$) of the search tree, and its utility $u(\mathcal{CS}^p(0)) = \sum_{C^p \in \mathcal{CS}^p(0)} u(C^p)$ is set as the initial optimal value.

4.3.3. Branching

Definition 10. **(Edge contraction)** As shown in Fig. 7, for an edge $(i, j) \in E_k^p$, edge contraction refers to merging the two coalitions C_i^p and C_j^p, connected by this edge, into a single coalition.

Starting from the current node t with structure $\mathcal{CS}_k^p(t)$, the algorithm selects a green edge (i, j) and evaluates whether contracting it satisfies the capacity constraint. If violated, the edge is marked red to indicate it cannot be contracted. Otherwise, the edge is contracted and then marked red to prevent redundant explorations. The resulting structure is given by

$$\mathcal{CS}_k^p(t+1) = \left(\mathcal{CS}_k^p(t) \backslash \left\{C_i^p, C_j^p\right\}\right) \cup \left\{C_i^p \cup C_j^p\right\} \tag{20}$$

The utility $u\left(\mathcal{CS}_k^p(t+1)\right)$ is then compared with the current optimal value, and the optimal value is updated if $u\left(\mathcal{CS}_k^p(t+1)\right)$ is greater.

4.3.4. Pruning

To avoid unnecessary computations, we design a bounding function $\xi(\cdot)$. If the bound for the current structure, $\xi\left(\mathcal{CS}_k^p\right)$, is lower than the current optimal utility, the branch is pruned to prevent further

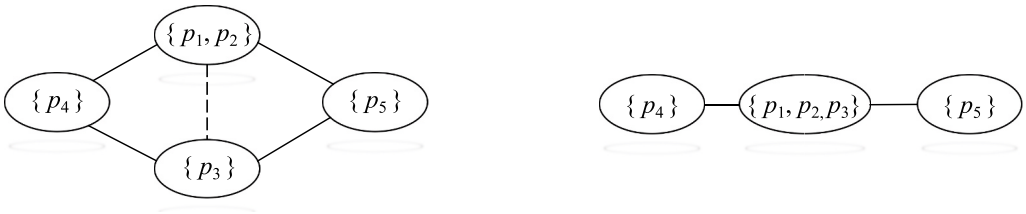

(a) Before contraction (b) After contraction

Fig. 7. Example of an edge contraction.

exploration of the subtree. Given the structure $\mathcal{CS}_k^p = \left\{C_1^p, C_2^p, \ldots, C_{|\mathcal{CS}_k^p|}^p\right\}$ where the coalitions are sorted in descending order of utility, i.e.,

$$u(C_1^p) \geq u(C_2^p) \geq \cdots \geq u\left(C_{|\mathcal{CS}_k^p|}^p\right) \tag{21}$$

the bounding function $\xi(\cdot)$ is defined as

$$\xi(\mathcal{CS}_k^p) = \sum_{i=1}^{\lceil |N_k^p|/\lambda \rceil} u(C_i^p) \tag{22}$$

where $\lceil |N_k^p|/\lambda \rceil$ is the minimum possible size of $\mathcal{CS}_k^p$.

Proposition 3. *For any passenger coalition structure $\mathcal{CS}_k^p$, the bounding function $\xi(\mathcal{CS}_k^p)$ provides an upper bound on the utility of any coalition structure $\mathcal{CS}_{b,k}^p$ within its subtree $\mathcal{ST}(\mathcal{CS}_k^p)$. Formally, $\forall \mathcal{CS}_{b,k}^p \in \mathcal{ST}(\mathcal{CS}_k^p)$: $\xi(\mathcal{CS}_k^p) \geq u\left(\mathcal{CS}_{b,k}^p\right)$.*

Proof. See Appendix B.

The bounding function $\xi(\cdot)$ is simple yet effective, significantly reducing the search space without sacrificing solution quality. Importantly, it relies only on monotonicity rather than superadditivity, making it well-suited for real-world applications.

5. Utility allocation

5.1. Operator utility allocation

Assumption 1 implies that, given an operator coalition structure $\mathcal{CS}^o$, each operator's utility depends on its own characteristics. These characteristics are quantified and incorporated into predefined allocation protocols. To ensure computational efficiency and align with operator behaviors, we propose the following allocation protocols.

5.1.1. Equal allocation

Equal allocation is the simplest protocol, distributing the total coalition utility evenly among operators, i.e.,

$$x_i = \frac{u(C^o)}{|C^o|}, \quad \forall i \in C^o \tag{23}$$

This ensures equal shares regardless of individual contributions and is effective when operator bargaining powers are relatively balanced.

5.1.2. Investment-based allocation

A more realistic allocation considers operator investment, i.e.,

$$x_i = \frac{w_i}{\sum_{j \in C^o} w_j} \cdot u(C^o), \quad \forall i \in C^o \tag{24}$$

where w_i denotes the investment weight of operator i, quantified by financial contributions or determined through negotiation. This approach allocates utility proportionally to each operator's bargaining power, reflecting their relative status within the coalition.

5.1.3. Performance-based allocation

Performance-based allocation distributes utility based on actual operational performance, i.e.,

$$x_i = \frac{\sum_{r \in O_i} d_{n_r^o n_r^\omega} + \sum_{v \in V_i} d\left(R_v^*\right)}{\sum_{j \in C^o}\left(\sum_{r \in O_j} d_{n_r^o n_r^\omega} + \sum_{v \in V_j} d\left(R_v^*\right)\right)} \cdot u(C^o), \quad \forall i \in C^o \tag{25}$$

where $O_i \subseteq N^p$ denotes the set of travel requests shared by operator i, and $V_i \subseteq \mathcal{CS}_*^p$ represents the set of passenger coalitions served by operator i's vehicles. Operators with higher request values and longer operating distances receive larger utility shares, incentivizing operators to actively share requests and vehicles.

Different protocols may be adopted depending on specific objectives, and each protocol can lead to a stable structure. In Section 6.4.2, we further explore how these protocols influence the stability of operator coalition structures.

5.2. Passenger utility allocation

Definition 4 indicates that a stable passenger coalition structure is one with an ϵ-kernel stable utility allocation. To achieve this, we employ the PK (payments in the kernel) algorithm to determine each passenger's utility (Bistaffa et al., 2017).

5.2.1. Allocation initialization

Within each passenger coalition $C^p \in \mathcal{CS}_*^p$, we initialize the allocation based on each passenger's solo travel distance and detour distance, i.e.,

$$y_i = \frac{d_i^{\text{solo}} - d_i^{\text{detour}}}{\sum_{j \in C^p}\left(d_j^{\text{solo}} - d_j^{\text{detour}}\right)} \cdot u(C^p) \tag{26}$$

where the solo travel distance is defined as $d_i^{\text{solo}} = d_{n_i^o n_i^\omega}$, the ride-pooling travel distance as $d_i^{\text{share}} = \sum_{k=r}^{l-1} d_{R_{C^p}^*[k], R_{C^p}^*[k+1]}$, and the detour distance as $d_i^{\text{detour}} = d_i^{\text{share}} - d_i^{\text{solo}}$.

5.2.2. Utility transfer

Starting from the initial allocation, utility is iteratively transferred between passenger pairs with the maximum surplus difference $\delta(C^p)$ until the stopping criterion $\delta(C^p)/u\left(\mathcal{CS}_*^p\right) \leq \epsilon$ is met. The maximum surplus difference is defined as

$$\delta(C^p) = \max_{i,j \in C^p}\left(s_{ij} - s_{ji}\right) \tag{27}$$

where s_{ij} denotes the surplus defined in Section 3.1.2. The total surplus difference across all coalitions $\sum_{C^p \in \mathcal{CS}^p} \delta(C^p)$ measures the overall stability of the passenger coalition structure.

In the original PK algorithm, the transfer amount is set as $\Delta u = \delta(C^p)/2$, eliminating the current maximum surplus difference. However, this approach does not ensure that the resulting utility y_j for passenger j remains above their individual utility when traveling alone. Thus, we

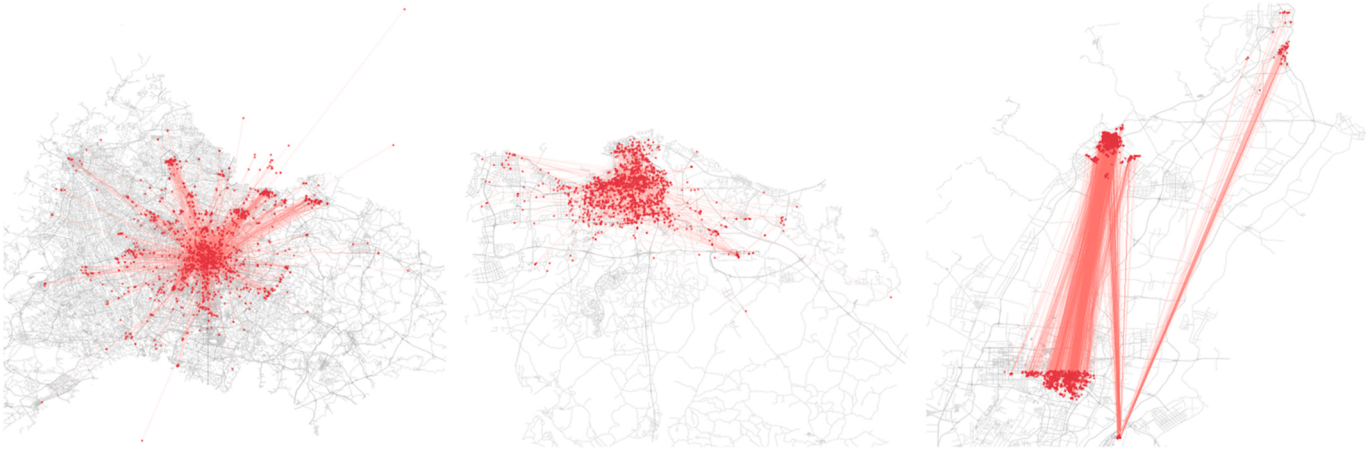

Fig. 8. Travel requests distribution (only 1000 requests are selected in each city for illustration).

modify the transfer amount to

$$\Delta u = \min\left\{\frac{\delta(C^p)}{2}, \max\left\{0, y_j - \frac{\delta(C^p)}{2} - u(\{p_j\})\right\}\right\} \tag{28}$$

Equation (28) guarantees that utility transfers occur only if the resulting utility of passenger j remains at least equal to their standalone utility $u(\{p_j\})$. This modification prevents passengers from leaving the CRP due to inadequate utility allocations.

When multiple passenger pairs (i, j) exhibit the same maximum surplus difference $\delta(C^p)$, a deterministic selection rule is employed to avoid potential oscillations: pairs are selected according to a fixed priority (e.g., lexicographical order of passenger indices) to ensure a unique pair (i, j) is chosen for each transfer step.

Proposition 4. *Given a passenger coalition structure $\mathcal{CS}^p_*$ and the corresponding utility values $\{u(C^p)\}_{C^p \in \mathcal{CS}^p_*}$, the modified PK algorithm produces an allocation $Y = \{y_i\}_{i \in N^p}$ after a finite number of steps that satisfies the following properties*:

- *ϵ-kernel stability, i.e.*, $\forall C^p \in \mathcal{CS}^p_* : \delta(C^p)/|u(\mathcal{CS}^p_*)| \leq \epsilon$
- *Individual rationality, i.e.*, $\forall i \in N^p$: $y_i \geq u(\{p_i\})$

Proof. See Appendix C.

6. Case study

6.1. Experimental setup

This study evaluates the proposed framework using real-world ride-hailing data from three representative regions in China: Chengdu, Haikou, and the Ningxia Hui Autonomous Region. Chengdu and Haikou represent typical urban environments, while the Ningxia Hui Autonomous Region, a provincial-level region, covers both intra-urban and intercity ride-pooling scenarios. For simplicity, "Ningxia" is used hereafter to refer to the Ningxia Hui Autonomous Region. The spatial distributions of travel requests' origins and destinations are shown in Fig. 8. These regions are selected to reflect diverse regional and request characteristics, particularly variations in travel distance distributions, as illustrated in Fig. 9. Specifically, the Chengdu dataset mainly includes medium-distance trips, Haikou has a high proportion of short-distance trips, and Ningxia primarily features longer trips. Such diversity allows for a comprehensive assessment of the proposed framework (see Fig. 10).

Due to limited real-world data on multiple operators within the same spatio-temporal window, operators are simulated for each region, with travel requests randomly assigned to them. To reflect market share differences, each operator is assigned a heterogeneous fleet size. Each operator's vehicles are distributed across road network nodes based on the historical distribution of travel requests, with allocation proportional to these density weights. Minor random variations are added to reflect dynamic dispatching changes. For each passenger coalition C^p, the nearest available vehicle from the operator coalition $f^{\rightarrow}_{p,o}(C^p)$ is assigned to provide service. We conducted a sensitivity analysis on the travel request allocation rule to demonstrate that the random allocation method does not affect the conclusions of this study (see Appendix D).

All experiments run on an Intel i5-12490F CPU (3.00 GHz) with 16 GB RAM. The experimental parameters are summarized in Table 1. The cost parameters, including fuel cost c^f, employment cost c^e, depreciation

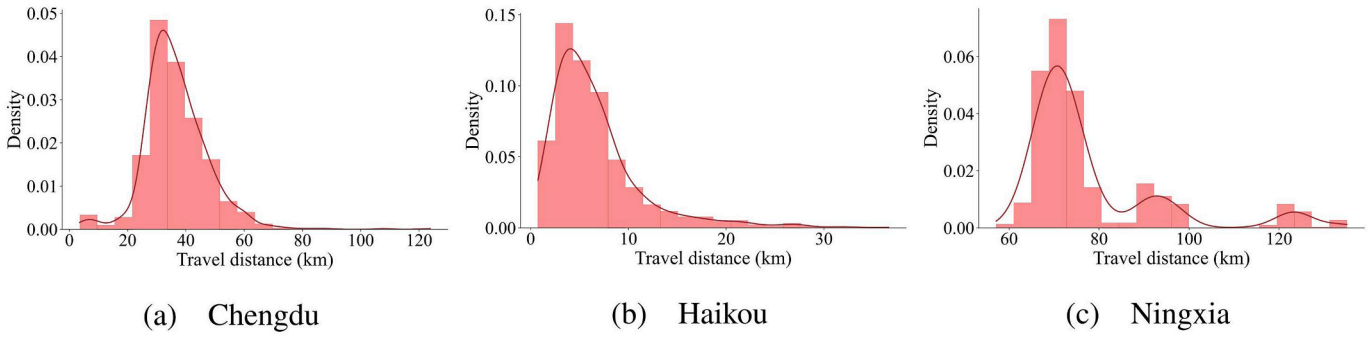

Fig. 9. Travel distance distribution.

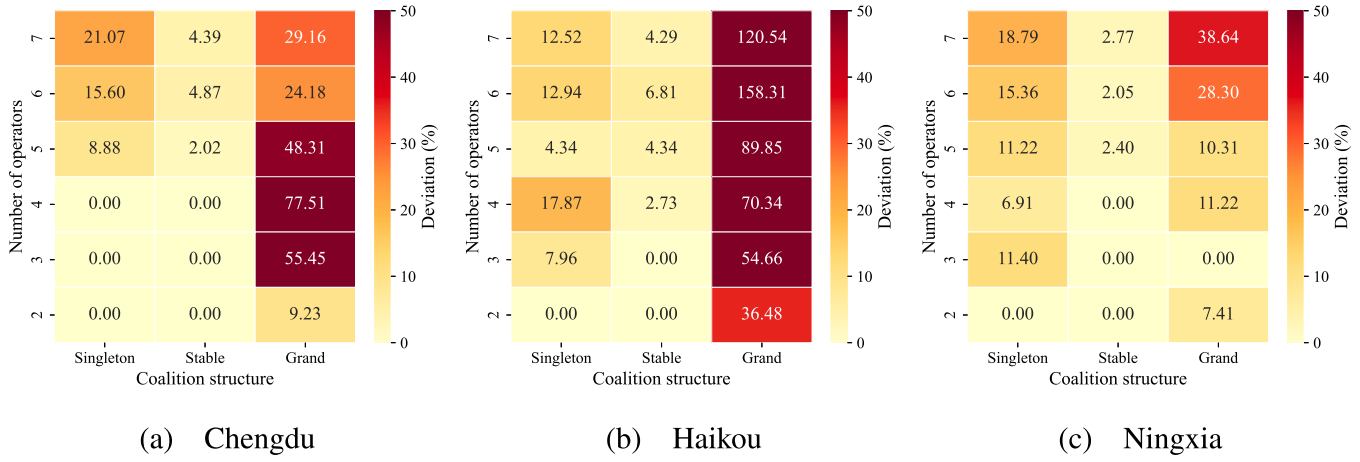

Fig. 10. Operator deviation rate.

Table 1
Parameter settings.

Notation	Definition	Value
c^f	Fuel cost per kilometer	0.2 (CNY/km)
c^e	Employment cost per kilometer	0.8 (CNY/km)
c^d	Depreciation cost per kilometer	0.2 (CNY/km)
ρ	Profit per kilometer	0.5 (CNY/km)
γ	Cooperative benefit parameter	3 (CNY/km)
λ	Vehicle capacity excluding the driver	4 (pax/veh)
ϵ	Convergence tolerance of CRP–CFSS	0.001
τ	Time limit in CRP–CFOS	60 s
—	Default allocation protocol for operators	Performance-based allocation

cost c^d, and profit parameter ρ, are based on average operating expenses and common pricing practices in China. Unless specified, operator utilities are allocated using the performance-based method. We set $\gamma = 3$ (CNY/km), which represents the marginal utility of distance reduction, i.e., the monetary value passengers attach to each kilometer of pooled distance saved. Chen et al. (2024) calibrated passengers' price and detour elasticity in nine Chinese cities, showing that when the detour is 10%–20%, passengers generally require a 10%–20% fare discount. This implies that in a 10 km trip with a fare of 30 CNY, avoiding an additional 2 km detour (20%) corresponds to a willingness to pay of about 6 CNY, or roughly 3 CNY per kilometer saved. We set $\tau = 40$ s to manage runtime. The impacts of these settings are further analyzed in the sensitivity tests in Section 6.

6.2. Dynamic coalition formation method

This section evaluates the core contribution of the study, i.e., dynamic coalition formation method for operators. We focus on three types of coalition structures:

- Singleton coalition structure: full competition scenario among operators, i.e., $\{\{o_i\}|o_i \in N^o\}$.
- Grand coalition structure: full cooperation strategy adopted by existing aggregation platforms, i.e., $\{N^o\}$.
- Stable coalition structure: dynamic coalition formation approach, i.e., $\mathcal{CS}^o_{\text{st}}$.

The results in Table 5 show that coalition formation improves operational efficiency. As the size of the operator coalition increases, the matching range between passenger demand and vehicle supply expands, which raises vehicle occupancy, reduces empty trips, and ultimately lowers total costs. Both the stable and grand coalition structures show significant improvements over the singleton structure. For example, in Chengdu, the stable coalition structure increases vehicle occupancy by 14.97% and reduces total costs by 10.68%, while the grand coalition structure increases occupancy by 28.05% and reduces costs by 14.83%. In Ningxia, similar trends are observed, while in Haikou, the stable coalition structure aligns with the singleton structure itself, resulting in identical metrics between the two.

However, the grand coalition structure faces significant stability challenges. Its deviation rate is notably high in Chengdu (48.31%), Haikou (89.85%), and Ningxia (10.31%), as shown in Table 2. This instability persists across all three payoff distribution schemes defined in Section 5.1. Under the equal split rule, large operators incur higher costs but receive the same allocation as small operators, giving them incentives to leave. Under the investment-based or performance-based rules, small operators often receive less than their standalone or subcoalition payoffs, discouraging participation. In other words, each allocation rule carries an inherent bias: equal split favors small operators, while investment- or performance-based schemes favor large ones. Therefore, the poor stability of the grand coalition is not a flaw of a particular allocation scheme, but the inevitable result of operator scale and cost heterogeneity.

By contrast, the stable coalition structure exhibits much lower deviation rates. This is because in the dynamic formation process, a coalition survives only when all members are better off than acting alone, so groups with strong conflicts are filtered out. Moreover, once most of the cooperation gains have already been realized in the stable structure, any further deviation can bring only limited additional benefits, which weakens the incentive to deviate. These factors explain why the deviation rates of the stable coalition remain low even though a SNE may not strictly exist.

These findings highlight that while larger coalitions bring efficiency gains, heterogeneity in operator size and cost makes the grand coalition

Table 2
Results for different operator coalition formation methods.

Region	$\mathcal{CS}^o$	Efficiency		Stability	
		Vehicle occupancy (%)	Total cost (CNY)	Number of deviation groups	Operator deviation rate (%)
Chengdu	Singleton	70.03	6810.38	7	8.88
	Stable	85.00	6085.81	3	2.02
	Grand	98.08	5800.64	23	48.31
Haikou	Singleton	63.75	2095.58	5	4.34
	Stable	63.75	2095.58	5	4.34
	Grand	91.07	1573.08	19	89.85
Ningxia	Singleton	91.07	4248.36	13	11.22
	Stable	98.08	3899.93	4	2.40
	Grand	98.08	3509.93	12	10.31

Note: Vehicle occupancy = total number of passengers/(number of passenger coalitions × vehicle capacity) × 100%; Number of deviation groups = $\left|\left\{i,j \in C^p, C^p \in \mathcal{CS}_*^p \middle| s_{ij} - s_{ji} > 0\right\}\right|$; Operator deviation rate = total deviation gain/total utility × 100%.

intrinsically unstable. The stable coalition offers a practicable compromise, retaining much of the efficiency benefit of cooperation while maintaining robustness in diverse operator environments.

6.3. Algorithm performance

In this section, we focus on validating the efficiency and robustness of the proposed algorithms for real-world applications. Since these experiments depend on data scale rather than specific regions, we only report results based on one dataset in Sections 6.3 and 6.4, without loss of generality. We select Ningxia's dataset as it includes both standard ride-pooling orders and intercity ride-pooling scenarios, making it more representative of diverse real-world use cases.

6.3.1. Overall performance

We evaluate the proposed algorithms across nine instances, each involving different combinations of operators and passengers. Since CRP-CFOS, CRP-CFSS, and PK algorithms all require the utilities of passenger coalitions, we maintain a global cache to store computed utilities and prevent redundant calculations. The experimental results are summarized in Table 3, with key performance metrics such as CPU (Central Processing Unit) time and deviation rates shown in Fig. 11.

At the operator level, CRP-CFOS consistently identifies stable coalition structures, achieving a maximum deviation rate of 3.52% and perfect stability (0%) for instances with $|N^o| = 5$. The number of possible operator coalitions is $B_5 = 52$, and each coalition C^o corresponds to a set of passenger coalitions bounded by the restricted Bell number $\widehat{B}_{|P|}$, which grows exponentially (e.g., on the order of 10^{100} for 106 passengers). This combinatorial explosion underlies the computational challenge, but the use of a global cache and a time limit τ keeps runtime manageable. Section 6.3.2 confirms that the time limit does not affect the final operator coalition structure.

At the passenger level, CRP-CFSS efficiently identifies optimal structures, achieving a 0% optimality gap within 7 min even for scenarios with 106 passengers. This performance is enabled by parallel processing on disjoint subgraphs and the pruning strategy of the bounding function $\xi(\cdot)$. The PK algorithm also ensures passenger stability, with deviation rates consistently below 0.05%, though its runtime increases with passenger numbers because its iterative utility transfer requires repeated recalculation of surplus differences across many pairs.

In summary, the proposed algorithms can efficiently handle hour-ahead requests with up to 5 operators and 106 passengers. For shorter planning horizons, the framework can be adapted to minute-ahead requests by reducing the batch size to around 30 passengers.

6.3.2. Sensitivity analysis of the time limit in CRP-CFOS

In each iteration t of CRP–CFOS, the computation of the optimal passenger coalition structure $\mathcal{CS}_*^p(t)$ is constrained by a time limit τ. To evaluate the impact of this constraint on the final operator coalition

Table 3
Performance metrics of different instances.

Algorithm	Instance	$\|N^o\| = 3$			$\|N^o\| = 4$			$\|N^o\| = 5$		
		$\|N^p\| = 28$	$\|N^p\| = 51$	$\|N^p\| = 86$	$\|N^p\| = 44$	$\|N^p\| = 67$	$\|N^p\| = 95$	$\|N^p\| = 51$	$\|N^p\| = 80$	$\|N^p\| = 106$
Operator level										
CRP–CFOS	Number of iterations	2	2	4	6	4	9	2	4	16
	Number of operator coalitions	2	2	2	3	3	2	3	3	3
	Total utility (CNY)	1385.46	2180.65	3565.62	2021.30	2833.48	4052.52	2425.67	3521.96	4623.95
	Total deviation gain (CNY)	12.14	0.01	41.30	12.14	16.77	142.60	0.01	0.01	98.70
	Operator deviation rate (%)	0.88	0.00	1.16	0.60	0.59	3.52	0.00	0.00	2.13
	CPU time (s)	251.14	427.74	429.96	742.13	916.13	864.12	1656.38	1893.50	1817.22
Passenger level										
CRP–CFSS	Number of passenger coalitions	7	13	22	11	17	24	13	20	27
	Total utility (CNY)	−1140.93	−2013.98	−3321.23	−1805.32	−2638.95	−3664.82	−2020.62	−3061.76	−3999.06
	Optimality gap (%)	0.00	0.00	0.00	0.00	0.00	0.00	0.00	0.00	0.00
	CPU time (s)	122.27	244.34	244.00	244.96	366.38	244.08	366.27	366.44	366.67
PK	Number of iterations	6.57	5.77	5.41	6.27	5.65	5.79	6.00	5.60	5.59
	Total surplus difference (CNY)	0.54	0.68	0.52	0.54	0.92	0.62	0.52	0.75	0.86
	Passenger deviation rate (%)	0.05	0.03	0.02	0.03	0.03	0.02	0.03	0.02	0.02
	CPU time (s)	9.99	83.52	1883.32	14.32	84.85	1948.40	15.70	320.36	1160.14
Overall										
CRP framework	CPU time (s)	383.40	755.59	2557.28	1001.41	1367.36	3056.59	2038.34	2580.30	3344.02

Note: Operator deviation rate = total deviation gain/total utility × 100%; Optimality gap = (optimal solution - total utility)/|optimal solution| × 100%; Number of iterations = total iterations/number of passenger coalitions; Passenger deviation rate = total surplus difference/|total utility| × 100%.

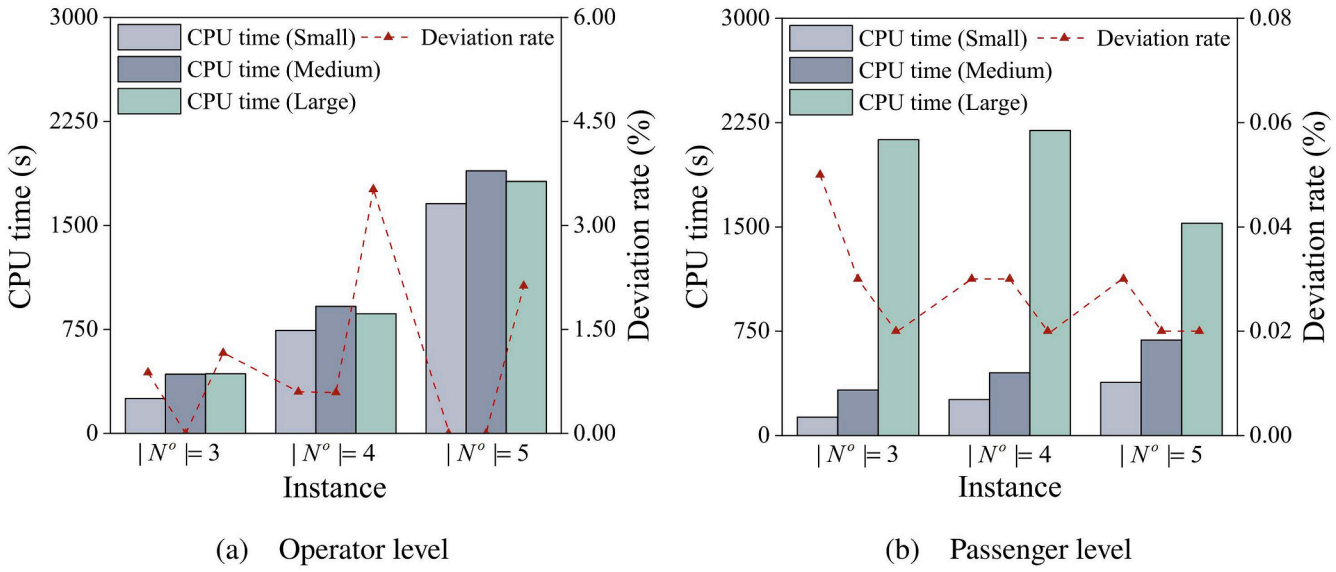

Fig. 11. CPU time and deviation rate of different instances. Small, medium, and large represent instances with small-scale, medium-scale, and large-scale passenger sizes, respectively.

structure, we perform a sensitivity analysis on the parameter τ. The results for the instance with $|N^o| = 4$, $|N^p| = 44$ are shown in Table 4.

Without a time limit ($\tau = \infty$), CRP–CFOS requires 7592.14 s to converge to the stable structure $\mathcal{CS}^o_{\text{st}} = \{\{1, 2\}, \{3\}, \{4\}\}$. In contrast, imposing a moderate time limit ($\tau = 60$ s) yields the same structure within only 741.62 s. Thus, a carefully selected τ effectively balances computational efficiency and solution quality. The optimal choice of τ may vary with the number of operators and passengers.

During iterations, the time limit leads to approximate utility calculations, which could influence structural adjustments and iteration counts. Nevertheless, CRP–CFOS consistently converges to the same stable coalition structure across all tested instances, indicating that intermediate approximation errors introduced by the time limit do not significantly affect the final outcome. Once $\mathcal{CS}^o_{\text{st}}$ is obtained, we recompute the optimal passenger coalition structure $\mathcal{CS}^p_*$ without time constraints, ensuring accurate final utilities and allocations.

6.3.3. Sensitivity analysis of the cooperative benefit parameter

The cooperative benefit parameter γ significantly influences the formation of operator coalitions. We perform sensitivity analyzes to evaluate its effect, as shown in Fig. 12. The results highlight a clear transition in utility as γ changes.

When $\gamma \leq 1$, the deviation rate decreases as γ increases, indicating that the utility function $u(\cdot)$ exhibits subadditivity. This occurs because merging operator coalitions leads to lower passenger payments, thereby reducing operators' incentives to cooperate. Consequently, operators prefer smaller coalitions, stabilizing at {{1}, {2}, {3}, {4}}. In contrast, when $\gamma > 1$, an increasing γ increases the deviation rate, reflecting superadditivity in $u(\cdot)$. The cooperative benefit compensates for reduced payments, encouraging operators to form larger coalitions. For example, when $\gamma = 1.5$, the stable structure transitions to {{1, 2}, {3}, {4}}, with cooperative benefits contributing 93.71 CNY out of the total utility of 1899.03 CNY. This finding highlights the importance of choosing an appropriate γ to align individual operator incentives with system-wide efficiency.

A notable observation is that within a suitable range of γ, the stable operator coalition structure remains consistent and the deviation rates remain consistently low (0.24%–1.85%). Nonetheless, the optimal γ should be calibrated based on specific operational contexts and real-world data.

6.4. System benefit

6.4.1. Operator coalition formation

To evaluate the impact of the dynamic coalition formation mechanism on system performance, we analyze various operator coalition structures $\mathcal{CS}^o \subseteq N^o$ in instances with $|N^o| = 3$, $|N^p| = 28$, $|N^o| = 4$, $|N^p| = 44$, and $|N^o| = 5$, $|N^p| = 51$. Results are presented in Fig. 13, with detailed metrics for the instance $|N^o| = 4$, $|N^p| = 44$ summarized in Table 5.

As expected, operator cooperation promotes more extensive ride-pooling, improving resource utilization and reducing operating costs. For example, the singleton coalition structure {{1}, {2}, {3}, {4}} has an average cost of 326.09 CNY, whereas the grand coalition structure {{1, 2, 3, 4}} reduces this cost to 308.23 CNY. Meanwhile, the stable structure {{1, 2}, {3}, {4}} achieves an average cost of 315.64 CNY, a 3.2% reduction compared to the independent-operation case. Passenger

Table 4
Sensitivity analysis of τ ($|N^o| = 4$, $|N^p| = 44$).

τ (s)	Number of iteration	CPU time of CRP-CFOS (s)	$\mathcal{CS}^o_{\text{st}}$
20	4	261.85	{{1, 2}, {3}, {4}}
30	2	386.98	{{2}, {1, 3}, {4}}
40	4	498.98	{{1, 2}, {3}, {4}}
50	6	626.29	{{1, 2}, {3}, {4}}
60	6	742.13	{{1, 2}, {3}, {4}}
120	6	1479.99	{{1, 2}, {3}, {4}}
180	6	2228.81	{{1, 2}, {3}, {4}}
240	6	2982.81	{{1, 2}, {3}, {4}}
∞	6	7592.14	{{1, 2}, {3}, {4}}

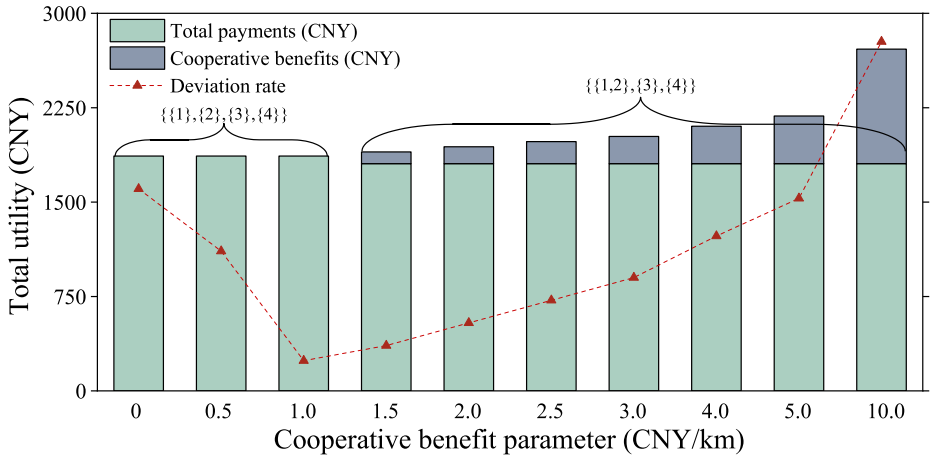

Fig. 12. Sensitivity analysis of γ ($|N^o| = 4$, $|N^p| = 44$).

payments drop from 42.41 to 41.03 CNY (3.3% reduction), and average travel distance decreases from 91.87 km/pax to 87.41 km/pax (4.9% reduction). However, the relationship between cooperation rate and cost reduction is not strictly linear. The structure {{1, 2}, {3}, {4}} with a cooperation rate of 33.25% achieves a cost of 315.64 CNY, whereas {{2, 3}, {1, 4}} with a higher cooperation rate (50%) results in a higher cost of 323.17 CNY. This indicates that the specific composition of operator coalitions critically influences the system benefits. Costs are guaranteed to decrease or remain unchanged only when coalitions are formed by merging existing coalitions. Similar patterns are observed in passenger payments and vehicle occupancy.

For passengers, increased operator cooperation generally reduces payments, but does not always reduce individual travel distances. For example, the structure {{1, 2, 3}, {4}} with 50% cooperation yields an average travel distance of 87.26 km/pax, while the grand coalition structure {{1, 2, 3, 4}} increases the average slightly to 90.94 km/pax. This highlights a trade-off between overall system efficiency and individual passenger convenience, as broader cooperation may require passengers to accept longer rides to benefit the system.

Deviation metrics further highlight the importance of dynamic coalition formation. In particular, these metrics are not directly correlated with the cooperation rate. For example, the stable structure {{1, 2}, {3}, {4}} has a low deviation rate of 0.6%, whereas the grand coalition structure {{1, 2, 3, 4}} exhibits a significantly higher deviation rate of 9.50%, with six operator groups incentivized to deviate.

6.4.2. *Operator utility allocation*

To assess the impact of operator utility allocation methods on system stability, we evaluate three allocation protocols (i.e., equal, investment-based, and performance-based) under fair allocation and stable allocation methods.

The fair allocation method, based on the grand coalition structure ({1, 2, 3, 4}), does not ensure stability. As shown in Table 6, the grand coalition structure results in significant deviation rates: 13.64% with the equal protocol, 27.10% with the investment-based protocol, and 8.72% with the performance-based protocol. This highlights the trade-off between fairness and stability, where simpler allocation methods tend to result in higher instability.

In contrast, the stable allocation method adjusts both the coalition structure and utilities iteratively to achieve stability. The coalition structure {{1, 2}, {3}, {4}} consistently emerges, with deviation rates as low as 0.60% under both the equal and performance-based protocols, and 5.01% under the investment-based protocol. This method effectively minimizes deviation incentives, ensuring much lower instability compared to fair allocation. Although stable coalition structures may differ across protocols, the key point is that the choice of protocol is not the focus of our study. Operators can negotiate their preferred protocol, and the approach guarantees convergence to a stable structure, ensuring satisfaction for all parties.

6.4.3. *Passenger utility allocation*

To evaluate passenger utility allocation methods, we similarly compare fair allocation and stable allocation. Both methods utilize the optimal passenger coalition structure but differ in utility distribution: fair allocation directly computes utilities using Eq. (26), whereas stable allocation iteratively seeks an ϵ-kernel stable distribution.

Results from Table 7 demonstrate that stable allocation substantially outperforms fair allocation in terms of stability. For example, in scenario $|N^o| = 3$, $|N^p| = 28$, fair allocation yields a deviation rate of 10.97% involving 38 deviation groups, while stable allocation achieves a deviation rate of just 0.05% with no deviation groups. Similar improvements are observed for other instances: deviation rates decrease from 11. 15% to 0. 03% for $|N^o| = 4$, $|N^p| = 44$ and from 9. 60% to 0. 03% for $|N^o| = 5$, $|N^p| = 51$.

7. Conclusions

This study develops a multi-level game framework that addresses the long-standing stability challenge in ride-pooling systems, especially under emerging aggregation platforms. Rather than relying on fixed cooperation or static matching rules, our framework enables dynamic, demand-driven coalition formation among operators and passengers. Through the case study, we demonstrate that stable and efficient matching outcomes can be achieved even in competitive and fragmented markets.

Beyond technical contributions, our findings provide several practical insights. First, we show that dynamic coalition formation driven by deviation incentives can achieve significantly higher stability compared to the grand coalition structure. This suggests that aggregation platforms do not need to enforce global request sharing among all participants. Allowing flexible subgroup cooperation may better align with individual incentives and promote sustainable participation. Second, our results indicate that stable utility allocations often differ from fair or proportional distributions. Platforms that focus solely on fairness may face high deviation risks. This highlights the need to distinguish between fairness and stability, and to design allocation rules that reflect actual contributions and behavioral incentives.

A key challenge of this study lies in two aspects of practical applicability. On one hand, the inherent combinatorial complexity of multi-level coalition formation—where the number of feasible operator and passenger coalition structures grows exponentially with the number of participants (e.g., Bell numbers for operator coalitions)—imposes

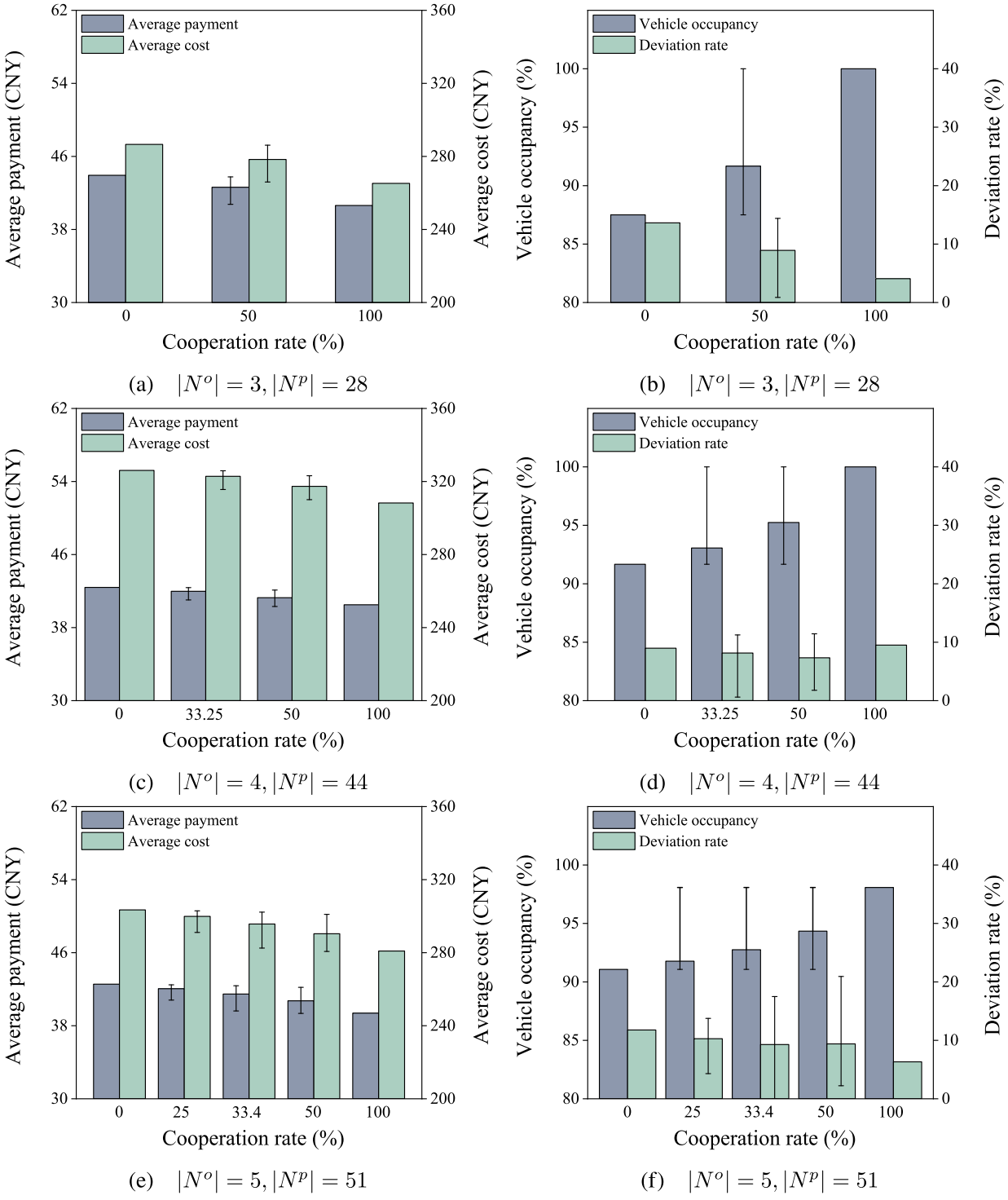

Fig. 13. Benefit metrics of different cooperation rates. Error bars represent the range of data, with upper and lower bounds indicating the maximum and minimum values, respectively.

fundamental limits on computational efficiency in large-scale scenarios. This complexity affects both coalition formation processes (such as CRP-CFOS) and utility allocation methods (including the PK algorithm), as even optimized approaches must navigate an exponentially expanding solution space. On the other hand, a simplifying assumption is adopted herein: empty-ride segments (i.e., the distance from vehicles' initial positions to the first passenger's pickup point) are omitted when calculating route costs. While this omission is intended to avoid over-complicating the core coalition formation logic, and is partially mitigated by the coalition's expanded vehicle supply (which helps reduce average empty-ride distances), it may still create discrepancies between the model's cost calculations and real-world dispatching expenses, particularly for short-distance ride-pooling trips.

Future work will focus on addressing these challenges to further enhance the framework's practical value: targeted approximation strategies and scalable heuristics will be developed to mitigate the combinatorial complexity of coalition formation; insights from studies exploring empty-ride distance distributions will be drawn upon to

Table 5
Benefit metrics of different operator coalition structures ($|N^o| = 4$, $|N^p| = 44$).

$\mathcal{CS}^o$	Cooperation rate (%)	Operator level			Passenger level		
		Average cost (CNY)	Number of deviation groups	Deviation rate (%)	Average payment (CNY)	Average travel distance (km/pax)	Vehicleoccupancy (%)
{{1}, {2}, {3}, {4}}	0.00	326.09	8	8.98	42.41	91.87	91.67
{{1, 2}, {3}, {4}}	33.25	315.64	2	0.60	41.03	87.41	100.00
{{2}, {1, 3}, {4}}	33.25	323.31	5	7.29	42.05	91.12	91.67
{{2}, {3}, {1, 4}}	33.25	325.86	9	10.22	42.38	92.38	91.67
{{1}, {2, 3}, {4}}	33.25	325.21	10	9.24	42.29	91.98	91.67
{{1}, {3}, {2, 4}}	33.25	324.58	12	11.24	42.21	92.81	91.67
{{1}, {2}, {3, 4}}	33.25	322.42	9	10.32	41.93	92.23	91.67
{{1, 2, 3}, {4}}	50.00	310.07	3	2.56	40.31	87.26	100.00
{{2, 3}, {1, 4}}	50.00	323.17	12	10.45	42.11	92.48	91.67
{{1, 3}, {2, 4}}	50.00	321.49	9	10.37	41.81	92.05	91.67
{{3}, {1, 2, 4}}	50.00	312.59	3	6.08	40.63	87.95	100.00
{{1, 2}, {3, 4}}	50.00	311.98	3	1.78	40.55	87.77	100.00
{{2}, {1, 3, 4}}	50.00	321.62	7	8.69	41.83	91.19	91.67
{{1}, {2, 3, 4}}	50.00	320.64	12	11.44	41.69	92.59	91.67
{{1, 2, 3, 4}}	100.00	308.23	6	9.50	40.05	90.94	100.00

Note: Cooperation rate = average coalition size/total number of operators × 100%, when the average coalition size equals 1, the cooperation rate is 0; Number of deviation groups = $\left|\left\{C_b^o \subseteq N^o \middle| g(C_b^o) > 0\right\}\right|$, where the deviation gain $g(C_b^o) = u(C_b^o) - \sum_{i \in C_b^o} x_i$; Vehicle occupancy = total number of passengers/(number of passenger coalitions × vehicle capacity) × 100%.

Table 6
Benefit metrics of different operator utility allocation methods ($|N^o| = 4$, $|N^p| = 44$).

Allocation method	Allocation protocol	$\mathcal{CS}^o$	Total utility (CNY)	Utility allocation (CNY)	Number of deviation groups	Deviation rate (%)
Fair allocation	Equal	{{1,2,3,4}}	1906.59	(476.65, 476.65, 476.65, 476.65)	6	13.64
	Investment-based	{{1,2,3,4}}	1906.59	(953.30, 476.65, 357.49, 119.16)	6	27.10
	Performance-based	{{1,2,3,4}}	1906.59	(431.71, 470.55, 382.88, 621.46)	7	8.72
Stable allocation	Equal	{{1,2},{3},{4}}	2021.30	(527.05, 527.05, 331.37, 635.83)	2	0.60
	Investment-based	{{1,2},{3},{4}}	2021.30	(702.73, 351.37, 331.37, 635.83)	6	5.01
	Performance-based	{{1,2},{3},{4}}	2021.30	(566.35, 487.75, 331.37, 635.83)	2	0.60

Table 7
Benefit metrics of different passenger utility allocation methods.

Instance	$\|N^o\| = 3$, $\|N^p\| = 28$		$\|N^o\| = 4$, $\|N^p\| = 44$		$\|N^o\| = 5$, $\|N^p\| = 51$	
Allocation method	Fair allocation	Stable allocation	Fair allocation	Stable allocation	Fair allocation	Stable allocation
Total utility (CNY)	−1140.93	−1140.93	−1805.32	−1776.77	−2020.62	−2020.83
Number of deviation groups	38	0	57	0	53	0
Deviation rate (%)	10.97	0.05	11.15	0.03	9.60	0.03

Note: Number of deviation groups = $\left|\left\{i,j \in C^p, C^p \in \mathcal{CS}_z^p \middle| s_{ij} - s_{ji} > 0\right\}\right|$.

integrate empty-ride costs into the route cost function; extend the framework to dynamic environments with rolling horizons and vehicle movement; and incorporate behavioral models under bounded rationality. Additionally, given the current reliance on simulated operator data due to the unavailability of real-world multi-operator data, future research will prioritize integrating real multi-operator data to better capture actual competitive dynamics. Notably, within our framework, "approximate stability" identifies the most stable configuration that can be obtained when exact SNE does not exist. Future work may refine this analysis by explicitly defining more relaxed stability concepts that are better suited to practical coalition formation.

CRediT authorship contribution statement

Yaotian Tan: Writing – review & editing, Writing – original draft, Visualization, Software, Methodology, Investigation, Formal analysis, Data curation, Conceptualization. **Shuyue Qian:** Visualization, Validation, Investigation, Formal analysis, Data curation. **Aoyong Li:** Writing – review & editing, Writing – original draft, Validation, Supervision, Resources, Project administration, Funding acquisition, Conceptualization. **Haiyang Yu:** Writing – review & editing, Validation, Supervision, Resources. **Jie Gao:** Writing – review & editing, Validation, Supervision, Methodology.

Replication and data sharing

The data and codes used in this study are available at https://doi.org/10.26599/ETSD.2025.9190057.

Declaration of competing interest

The authors declare that they have no known competing financial interests or personal relationships that could have appeared to influence the work reported in this paper.

Acknowledgements

This research has been supported by the Young Scientists Fund of the National Natural Science Foundation of China (No. 52202389), the National Natural Science Foundation of China (No. T2588101), and the Fundamental Research Funds for the Central Universities.

Appendix A

Proposition 2. *For any two passenger coalitions C_1^p and C_2^p with $C_1^p \subseteq C_2^p$, it holds that $u(C_1^p) \geq u(C_2^p)$.*

Proof. Recall that

$$u(C^p) = -\left(c\left(R^*_{C^p}\right) + \rho \cdot \sum_{i \in C^p} d_{n_i^o n_i^w}\right) \tag{A1}$$

where $c\left(R^*_{C^p}\right) = \left(c^f + c^e + c^d\right) \cdot d\left(R^*_{C^p}\right)$ represents the total operating cost, and $\rho > 0$ denotes the profit parameter. By definition, the total operating cost $c\left(R^*_{C^p}\right)$ is linearly proportional to route distance, i.e.,

$$\frac{\partial c\left(R^*_{C^p}\right)}{\partial d\left(R^*_{C^p}\right)} = c^f + c^e + c^d \geq 0 \tag{A2}$$

When expanding a coalition from C_1^p to C_2^p, the optimal route for C_2^p remains the same as for C_1^p or is extended to accommodate additional passengers, we have

$$C_1^p \subseteq C_2^p \Rightarrow R^*_{C_1^p} \subseteq R^*_{C_2^p} \Rightarrow d\left(R^*_{C_1^p}\right) \leq d\left(R^*_{C_2^p}\right) \tag{A3}$$

Combining Eqs. (A2) and (A3), we have

$$c\left(R^*_{C_2^p}\right) \geq c\left(R^*_{C_1^p}\right) \tag{A4}$$

The term $\rho \sum_{i \in C^p} d_{n_i^o n_i^w}$ also increases as passengers are added to the coalition, i.e.,

$$\rho \sum_{i \in C_2^p} d_{n_i^o n_i^w} = \rho \left(\sum_{i \in C_1^p} d_{n_i^o n_i^w} + \sum_{i \in C_2^p \setminus C_1^p} d_{n_i^o n_i^w}\right) \geq \rho \sum_{i \in C_1^p} d_{n_i^o n_i^w} \tag{A5}$$

Combining Eqs. (A4) and (A5), we have

$$u(C_1^p) = -c\left(R^*_{C_1^p}\right) - \rho \sum_{i \in C_1^p} d_{n_i^o n_i^w} \geq -c\left(R^*_{C_2^p}\right) - \rho \sum_{i \in C_2^p} d_{n_i^o n_i^w} = u(C_2^p) \tag{A6}$$

which completes the proof.

Appendix B

Proposition 3. *For any passenger coalition structure $\mathcal{CS}_k^p$, the bounding function $\xi\left(\mathcal{CS}_k^p\right)$ provides an upper bound on the utility of any coalition structure $\mathcal{CS}_{b,k}^p$ within its subtree $\mathcal{ST}\left(\mathcal{CS}_k^p\right)$. Formally, $\forall \mathcal{CS}_{b,k}^p \in \mathcal{ST}\left(\mathcal{CS}_k^p\right) : \xi\left(\mathcal{CS}_k^p\right) \geq u\left(\mathcal{CS}_{b,k}^p\right)$*

Proof. Recall that

$$\xi\left(\mathcal{CS}_k^p\right) = \sum_{i=1}^{\lceil \frac{n_k}{\lambda} \rceil} u\left(C_{i,k}^p\right) \tag{B1}$$

where the coalitions are sorted in descending order of utility, i.e., $u\left(C_{1,k}^p\right) \geq u\left(C_{2,k}^p\right) \geq \ldots \geq u\left(C^p_{\left|\mathcal{CS}_k^p\right|,k}\right)$. Suppose that $\mathcal{CS}_{b,k}^p \in \mathcal{ST}\left(\mathcal{CS}_k^p\right)$ is also sorted in descending order of utility, i.e., $\mathcal{CS}_{b,k}^p = \left\{\widehat{C}_{1,k}^p, \widehat{C}_{2,k}^p, \ldots, \widehat{C}^p_{\left|\mathcal{CS}_{b,k}^p\right|,k}\right\}$, where $u\left(\widehat{C}_{1,k}^p\right) \geq u\left(\widehat{C}_{2,k}^p\right) \geq \cdots \geq u\left(\widehat{C}^p_{\left|\mathcal{CS}_k^p\right|,k}\right)$. For any $\widehat{C}_{i,k}^p, \widehat{C}_{j,k}^p \in \mathcal{CS}_{b,k}^p (i \neq j)$, there always exist $C^p_{r_i,k}, C^p_{r_j,k} \in \mathcal{CS}_k^p$, such that

$$\widehat{C}_{i,k}^p \supseteq C^p_{r_i,k}, \quad \widehat{C}_{j,k}^p \supseteq C^p_{r_j,k} \tag{B2}$$

with $r_i \neq r_j$. In other words, each coalition $\widehat{C}_{i,k}^p$ *in* $\mathcal{CS}_{b,k}^p$ can be traced back to at least one distinct source coalition $C^p_{r_i,k}$ in $\mathcal{CS}_k^p$. From Proposition 1, we

have

$$u\left(\widehat{C}^p_{i,k}\right) \le u\left(C^p_{r_i,k}\right), \quad \forall i \in \left\{1,2,..,\left|\mathcal{CS}^p_{b,k}\right|\right\} \tag{B3}$$

where $|\mathcal{CS}^p_{b,k}| \ge \lceil \frac{n_k}{\lambda} \rceil$. Then we have

$$\sum_{i=1}^{\lceil \frac{n_k}{\lambda} \rceil} u\left(\widehat{C}^p_{i,k}\right) \le \sum_{i=1}^{\lceil \frac{n_k}{\lambda} \rceil} u\left(C^p_{r_i,k}\right) \tag{B4}$$

Due to $\forall i,j \in \left\{1,2,..,\left|\mathcal{CS}^p_{b,k}\right|\right\} \wedge i \ne j : r_i \ne r_j$, we have

$$\sum_{i=1}^{\lceil \frac{n_k}{\lambda} \rceil} u\left(C^p_{i,k}\right) \ge \sum_{i=1}^{\lceil \frac{n_k}{\lambda} \rceil} u\left(C^p_{r_i,k}\right) \tag{B5}$$

Combining Eqs. (B4) and (B5), we have

$$\xi(\mathcal{CS}^p_k) = \sum_{i=1}^{\lceil \frac{n_k}{\lambda} \rceil} u\left(C^p_{i,k}\right) \ge \sum_{i=1}^{\lceil \frac{n_k}{\lambda} \rceil} u\left(C^p_{r_i,k}\right) \ge \sum_{i=1}^{\lceil \frac{n_k}{\lambda} \rceil} u\left(\widehat{C}^p_{i,k}\right) \ge \sum_{i=1}^{\left|\mathcal{CS}^p_{b,k}\right|} u\left(\widehat{C}^p_{i,k}\right) = u\left(\mathcal{CS}^p_{b,k}\right) \tag{B6}$$

which completes the proof.

Appendix C

Proposition 4. *Given a passenger coalition structure $\mathcal{CS}^p_*$ and the corresponding utility values $\{u(C^p)\}_{C^p \in \mathcal{CS}^p_*}$, the modified PK algorithm produces an allocation $Y = \{y_i\}_{i \in N^p}$ after a finite number of steps that satisfies the following properties*:

- *ϵ-kernel stability, i.e.*, $\forall C^p \in \mathcal{CS}^p_* : \delta(C^p)/|u(\mathcal{CS}^p_*)| \le \epsilon$.
- *Individual rationality, i.e.*, $\forall i \in N^p$: $y_i \ge u(\{p_i\})$.

Proof. We prove the two properties in turn.

(1) **ϵ-kernel stability**

Recall that for any $i, j \in C^p$, the perceived surplus difference is defined as

$$s_{ij} = y_i - u(\{p_i\}) - \left(y_j - u\left(\{p_j\}\right)\right) \tag{C1}$$

and the maximum surplus difference within coalition C^p is

$$\delta(C^p) = \max_{i,j \in C^p} \left(s_{ij} - s_{ji}\right) \tag{C2}$$

To avoid oscillations when multiple pairs have the maximum surplus difference, the algorithm employs a deterministic selection rule: when multiple (i, j) pairs satisfy $s_{ij} - s_{ji} = \delta(C^p)$, a unique pair (i^*, j^*) is selected via fixed priority (e.g., lexicographically smallest indices). Let $\delta_k = \delta(C^p)$ denote the maximum surplus difference at the k-th iteration, and let $S_k = \{(i, j) | s_{ij} - s_{ji} = \delta_k\}$ be the set of pairs with maximum surplus difference at iteration k.

For the selected pair $(i^*, j^*) = \sigma(S_k)$, the transfer amount $\Delta u_k > 0$ (positive by the transfer rule, as otherwise the algorithm would terminate) leads to

$$\begin{aligned} s_{i^* j^*}(k+1) - s_{j^* i^*}(k+1) &= \left[s_{i^* j^*}(k) + \Delta u_k\right] - \left[s_{j^* i^*}(k) - \Delta u_k\right] \\ &= \delta_k - 2\Delta u_k < \delta_k \end{aligned} \tag{C3}$$

For other pairs $(i, j) \in S_k \backslash \{(i^*, j^*)\}$, their surplus difference remains δ_k in this iteration, so the maximum surplus difference at iteration $k+1$ satisfies

$$\begin{aligned} \delta_{k+1} &= \max_{(i,j)} \left[s_{ij}(k+1) - s_{ji}(k+1)\right] \\ &= \max\{\delta_k, \delta_k - 2\Delta u_k\} = \delta_k \end{aligned} \tag{C4}$$

with $S_{k+1} = S_k \backslash \{(i^*, j^*)\}$ since the adjusted pair is no longer in the maximum set.

Let the coalition size be n (finite), so the total number of feasible (i, j) pairs is bounded by $n(n-1)$, making $|S_k|$ finite for all k. If $|S_k| = 1$, then $S_{k+1} = \varnothing$, and

$$\delta_{k+1} = \max\left\{s_{ij}(k+1) - s_{ji}(k+1) \middle| (i,j) \notin S_k\right\} < \delta_k \tag{C5}$$

because the only pair with maximum surplus difference has been adjusted. If $|S_k| > 1$, then $|S_{k+1}| = |S_k| - 1$ as the selected pair is removed; repeating this process, after $|S_k|$ iterations, there exists k' where $|S_{k'}| = 1$, leading to $\delta_{k'+1} < \delta_{k'}$.

Since $\{\delta_k\}$ is a non-increasing sequence (remaining constant only finitely many times) with a lower bound of 0, and each strict decrease has a

positive step size $2\Delta u_k$, there exists m such that $\delta_m \le \epsilon|u(\mathcal{CS}_*^p)|$, ensuring the algorithm terminates without oscillations and satisfies ϵ–kernel stability.

(2) **Individual rationality**

Individual rationality is proven by induction. In the base case, the initial allocation (defined in Eq. (26)) satisfies $y_i^{(0)} > 0 \ge u(\{p_i\})$ *for all* $i \in C^p$, *as each* $y_i^{(0)}$ is proportional to individual savings and $u(C^p) \ge 0$. Assume the allocation at step t satisfies $y_i^{(t)} \ge u(\{p_i\})$ for all $i \in C^p$. At step $t+1$, the transfer amount from j to i is

$$\Delta u = \min\left\{\frac{\delta(C^p)}{2},\ \max\left\{0,\ y_j^{(t)} - \frac{\delta(C^p)}{2} - u(\{p_j\})\right\}\right\} \tag{C6}$$

so the updated allocations satisfy:

$$\begin{aligned} y_j^{(t+1)} &= y_j^{(t)} - \Delta u \ge y_j^{(t)} - \left(y_j^{(t)} - \frac{\delta(C^p)}{2} - u(\{p_j\})\right) \\ &= \frac{\delta(C^p)}{2} + u(\{p_j\}) \ge u(\{p_j\}) \end{aligned} \tag{C7}$$

$$y_i^{(t+1)} = y_i^{(t)} + \Delta u \ge y_i^{(t)} \ge u(\{p_i\}) \tag{C8}$$

By induction, individual rationality holds throughout the algorithm. Since the process terminates in finite steps, the final allocation satisfies all stated properties, which completes the proof.

Appendix D

To examine whether the random request-allocation assumption may overstate the benefits of cooperation, we conduct a biased allocation experiment on the Ningxia dataset. The study area is divided into 1 km × 1 km grids. Starting from the cell with the highest demand density, adjacent cells are added until the cumulative demand reaches a share α of the city total (here $\alpha \in [20\%, 40\%]$). This defines the hotspot. In the biased scenarios, requests within the hotspot are allocated to Operator 1 with probability p (here $p \in [60\%, 90\%]$), while remaining requests are randomly allocated. Here, α denotes the share of requests contained in the hotspot relative to the whole area, and p denotes the probability that hotspot requests are preferentially allocated to Operator 1.

Table D1 reports the stable coalition structures and performance indicators under different allocation rules. As the bias increases, the stable coalition changes: under mild bias (B1) it remains the same as in the random case, while under stronger bias (B2–B4) Operator 1 tends to operate independently and the others are more likely to merge. Vehicle occupancy and total cost show only small fluctuations across scenarios. The number of deviation groups and the deviation rate rise as the bias becomes stronger, and the deviation rates remain at a relatively low level. Overall, cooperation still emerges under biased allocations and efficiency gains persist. The specific stable coalition structure, however, may differ depending on the competitive environment.

Table D1
Sensitivity analysis of request allocation rules.

Request allocation rule	Stable coalition structure	Vehicle occupancy (%)	Total cost (CNY)	Number of deviation groups	Deviation rate (%)
Random (baseline)	{{1, 2}, {3, 4}}	98.08	3899.93	4	2.40
Biased B1 ($\alpha = 20\%, p = 60\%$)	{{1, 2}, {3, 4}}	98.08	3912.47	5	2.75
Biased B2 ($\alpha = 30\%, p = 70\%$)	{{1}, {2, 3}, {4}}	97.15	3936.81	5	2.88
Biased B3 ($\alpha = 30\%, p = 80\%$)	{{1}, {2, 3, 4}}	96.94	3974.36	6	3.05
Biased B4 ($\alpha = 40\%, p = 90\%$)	{{1}, {2, 3, 4}}	96.43	4008.29	6	4.72

References

Alonso-González, M.J., Cats, O., van Oort, N., Hoogendoorn-Lanser, S., Hoogendoorn, S., 2020. What are the determinants of the willingness to share rides in pooled on-demand services. Transportation 48, 1733–1765.

Berend, D., Tassa, T., 2010. Improved bounds on Bell numbers and on moments of sums of random variables. Probab. Math. Stat. 30, 185–205.

Bistaffa, F., Farinelli, A., Cerquides, J., Rodriguez-Aguilar, J., Ramchurn, S.D., 2014. Anytime coalition structure generation on synergy graphs. In: International Conference on Autonomous Agents and Multiagent Systems, pp. 13–20.

Bistaffa, F., Farinelli, A., Chalkiadakis, G., Ramchurn, S.D., 2015a. Recommending fair payments for large-scale social ridesharing. In: ACM Conference on Recommender Systems, pp. 139–146.

Bistaffa, F., Farinelli, A., Chalkiadakis, G., Ramchurn, S.D., 2017. A cooperative game-theoretic approach to the social ridesharing problem. Artif. Intell. 246, 86–117.

Bistaffa, F., Farinelli, A., Ramchurn, S.D., 2015b. Sharing rides with friends: a coalition formation algorithm for ridesharing. In: Proceedings of the AAAI Conference on Artificial Intelligence, pp. 608–614.

Cai, Z., Chen, Y., Mo, D., Liu, C., Chen, X.M., 2024. Competition and evolution in ride-hailing market: a dynamic duopoly game model. Transport. Res. C Emerg. Technol. 164, 104665.

Chalkiadakis, G., Greco, G., Markakis, E., 2016. Characteristic function games with restricted agent interactions: Core-stability and coalition structures. Artif. Intell. 232, 76–113.

Chau, S.C.-K., Shen, S., Zhou, Y., 2022. Decentralized ride-sharing and vehicle-pooling based on fair cost-sharing mechanisms. IEEE Trans. Intell. Transport. Syst. 23, 1936–1946.

Chen, W., Huang, G., Ke, J., 2024. Development dilemma of ride-sharing: revenue or social welfare? arXiv:2412.08801.

Chremos, I.V., Malikopoulos, A.A., 2021. Design and stability analysis of a shared mobility market. In: European Control Conference, pp. 375–380.

Cui, Y., Makhija, R.S.M.S., Chen, R.B., He, Q., Khani, A., 2020. Understanding and modeling the social preferences for riders in rideshare matching. Transportation 48, 1809–1835.

Davis, M., Maschler, M., 1965. The kernel of a cooperative game. Nav. Res. Logist. 12, 223–259.

Deng, X., Papadimitriou, C.H., 1994. On the complexity of cooperative solution concepts. Math. Oper. Res. 19, 257–266.

Feng, S., Chen, T., Zhang, Y., Ke, J., Zheng, Z., Yang, H., 2024. A multi-functional simulation platform for on-demand ride service operations. Commun Transp Res 4, 100141.

Fielbaum, A., Kucharski, R., Cats, O., Alonso-Mora, J., 2022. How to split the costs and charge the travellers sharing a ride? Aligning system's optimum with users' equilibrium. Eur. J. Oper. Res. 301, 956–973.

Gao, J., Wong, T., Selim, B., Wang, C., 2022. VOMA: a privacy-preserving matching mechanism design for community ride-sharing. IEEE Trans. Intell. Transport. Syst. 23, 23963–23975.

Greco, G., Malizia, E., Palopoli, L., Scarcello, F., 2011. On the complexity of core, kernel, and bargaining set. Artif. Intell. 175, 1877–1910.
Hou, L., Geng, S., Kong, W., 2025a. Competition and cooperation in ride-sharing platforms: a game theoretic analysis of C2C and B2C aggregation strategies. Sustainability 17.
Hou, S., Wang, C., Gao, J., 2025b. Reinforced stable matching for crowd-sourced delivery systems under stochastic driver acceptance behavior. Transport. Res. C Emerg. Technol. 170, 104916.
Ke, H., Guo, Y., Liu, H., Li, H., 2025. A dynamic stable multi-rider ridesharing matching model considering the fairness of cost savings allocation. Transportmetrica 1–31.
Ke, J., Yang, H., Zheng, Z., 2020. On ride-pooling and traffic congestion. Transp. Res. Part B Methodol. 142, 213–231.
Ke, J., Zheng, Z., Yang, H., Ye, J., 2021. Data-driven analysis on matching probability, routing distance and detour distance in ride-pooling services. Transport. Res. C Emerg. Technol. 124, 102922.
Klusch, M., Shehory, O., 1996. A polynomial kernel-oriented coalition algorithm for rational information agents. In: International Conference on Multi-Agent Systems, pp. 157–164.
Li, W., Pu, Z., Li, Y., Jeff, Ban X., 2019. Characterization of ridesplitting based on observed data: a case study of Chengdu, China. Transport. Res. C Emerg. Technol. 100, 330–353.
Li, X., Ke, J., Yang, H., Wang, H., Zhou, Y., 2024. An aggregate matching and pick-up model for mobility-on-demand services. Transp. Res. Part B Methodol. 190, 103070.
Liu, B., Zhao, X., Gu, Q., 2024. Pricing strategy and platform competition with partial multi-homing agents: when the aggregation platform exists in ride-sharing market. Transp. Res. Part E Logist Transp Rev 184, 103483.
Liu, H., Devunuri, S., Lehe, L., Gayah, V.V., 2023. Scale effects in ridesplitting: a case study of the City of Chicago. Transp. Res. Part A Policy Pract 173, 103690.
Liu, Y., Jia, R., Ye, J., Qu, X., 2022. How machine learning informs ride-hailing services: a survey. Commun Transp Res 2, 103545.
Lu, W., Quadrifoglio, L., 2019. Fair cost allocation for ridesharing services – modeling, mathematical programming and an algorithm to find the nucleolus. Transp. Res. Part B Methodol. 121, 41–55.
Ma, L., Tao, Z., Wei, Q., Huo, B., 2025. Cooperate with aggregation platform or not? Optimal decision for the on-demand ride service platform. Res. Transp. Bus. Manag. 59, 101251.
MOT, 2024. Regulatory information interaction system for online ride-hailing: october 2024 industry operation overview. https://zs.mot.gov.cn/mot/s.
Nourinejad, M., Roorda, M.J., 2016. Agent based model for dynamic ridesharing. Transport. Res. C Emerg. Technol. 64, 117–132.
Peng, Z., Shan, W., Jia, P., Yu, B., Jiang, Y., Yao, B., 2020. Stable ride-sharing matching for the commuters with payment design. Transportation 47, 1–21.
Sandholm, T., Larson, K., Andersson, M., Shehory, O., Tohmé, F., 1999. Coalition structure generation with worst case guarantees. Artif. Intell. 111, 209–238.
Tae, H., Kim, B.-I., Park, J., 2020. Finding the nucleolus of the vehicle routing game with time windows. Appl. Math. Model. 80, 334–344.
Tang, L., Liu, Z., Zhang, R., Duan, Z., Liang, Y., 2022. Who will travel with me? Personalized ranking using attributed network embedding for pooling. IEEE Trans. Intell. Transport. Syst. 23, 12311–12327.
Wang, X., Agatz, N., Erera, A., 2018. Stable matching for dynamic ride-sharing systems. Transp. Sci. 52, 850–867.
Wei, S., Feng, S., Ke, J., Yang, H., 2022. Calibration and validation of matching functions for ride-sourcing markets. Commun Transp Res 2, 100058.
Wooldridge, M., 2011. Agent and Multi-Agent Systems: Technologies and Applications. Springer Berlin Heidelberg, Berlin, Germany.
Yao, R., Bekhor, S., 2023. A general equilibrium model for multi-passenger ridesharing systems with stable matching. Transp. Res. Part B Methodol. 175, 102775.
Zhang, H., Zhao, J., 2019. Mobility sharing as a preference matching problem. IEEE Trans. Intell. Transport. Syst. 20, 2584–2592.
Zhou, Y., Yang, H., Ke, J., Wang, H., Li, X., 2022. Competition and third-party platform-integration in ride-sourcing markets. Transp. Res. Part B Methodol. 159, 76–103.
Zhu, P., Mo, H., 2022. The potential of ride-pooling in VKT reduction and its environmental implications. Transp. Res. D Transp. Environ. 103, 103155.

Yaotian Tan is currently pursuing the M.S. degree with the State Key Laboratory of Intelligent Transportation System, Beihang University, China. His research interests include integrated transportation and shared mobility.

Shuyue Qian is currently pursuing the M.S. degree with the State Key Laboratory of Intelligent Transportation System, Beihang University, China. His research interests include low-altitude economy and shared mobility.

Aoyong Li is an Associate Professor at the State Key Laboratory of Intelligent Transportation System, Beihang University, China. His research interests include intelligent transportation systems, transportation data mining, and shared micro-mobility.

Haiyang Yu is a Professor at the State Key Laboratory of Intelligent Transportation System, Beihang University, China. His research interests include traffic big data, traffic control, and intelligent vehicle infrastructure cooperative systems.

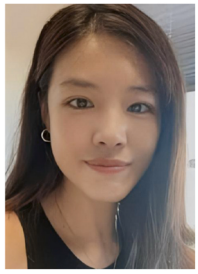

Jie Gao is an Assistant Professor at the Department of Transport & Planning, TU Delft, the Netherlands. Her research combines artificial intelligence, operations research, and microeconomics to study uncertainty, real-time decisions, and decentralized coordination in shared mobility.